

1966

# Hydrolysis products of rare earth silicides

Dale Dean Clyde  
*Iowa State University*

Follow this and additional works at: <https://lib.dr.iastate.edu/rtd>

 Part of the [Physical Chemistry Commons](#)

## Recommended Citation

Clyde, Dale Dean, "Hydrolysis products of rare earth silicides " (1966). *Retrospective Theses and Dissertations*. 5352.  
<https://lib.dr.iastate.edu/rtd/5352>

This Dissertation is brought to you for free and open access by the Iowa State University Capstones, Theses and Dissertations at Iowa State University Digital Repository. It has been accepted for inclusion in Retrospective Theses and Dissertations by an authorized administrator of Iowa State University Digital Repository. For more information, please contact [digirep@iastate.edu](mailto:digirep@iastate.edu).

This dissertation has been  
microfilmed exactly as received 67-5574

CLYDE, Dale Dean, 1938-  
HYDROLYSIS PRODUCTS OF RARE EARTH SILICIDES.

Iowa State University of Science and Technology, Ph.D., 1966  
Chemistry, physical

University Microfilms, Inc., Ann Arbor, Michigan

HYDROLYSIS PRODUCTS OF RARE EARTH SILICIDES

by

Dale Dean Clyde

A Dissertation Submitted to the  
Graduate Faculty in Partial Fulfillment of  
The Requirements for the Degree of  
DOCTOR OF PHILOSOPHY

Major Subject: Physical Chemistry

Approved:

Signature was redacted for privacy.

~~In Charge~~ of Major Work

Signature was redacted for privacy.

~~Head~~ of Major Department

Signature was redacted for privacy.

~~Dean~~ of Graduate College

Iowa State University  
Of Science and Technology  
Ames, Iowa

1966

## TABLE OF CONTENTS

	Page
INTRODUCTION	1
LITERATURE REVIEW	3
Rare Earth Silicides	3
Silanes	14
Hydrolysis of Rare Earth Carbides	23
EXPERIMENTAL PROCEDURES	29
Preparation of the Rare Earth Silicides	29
Preparation of the Silanes	30
Separation and Identification of the Silanes	37
CALCULATIONS	45
RESULTS	47
Rare Earth Silicides	47
Mass Spectra of the Silanes	47
Relative Molar Response. for the Silanes	65
Hydrolysis Products of the Rare Earth Silicides	70
DISCUSSION	74
Relative Molar Response	74
Mass Spectra of the Silanes	79
Hydrolysis Reactions of the Rare Earth Silicides	84
SUMMARY	89
BIBLIOGRAPHY	90
ACKNOWLEDGMENTS	97
APPENDIX	98

Calculations for the Thermal Conductivities  
of the Silanes

page

98

## LIST OF FIGURES

	Page
Figure 1. The crystal structure of $\text{ThSi}_2$ (Wells, 1962, p. 822)	11-13
Figure 2. The crystal structure of $\text{AlB}_2$ . The smaller circles represent B atoms (Wells, 1962, p. 774)	11-13
Figure 3. A-layer of metal atoms (Aronsson, Lundstrom and Rundqvist, 1965, p. 60)	11-13
Figure 4. $\text{U}_3\text{Si}_2$ structure projected on the basal plane. The large circles represent the silicon atoms (Aronsson, Lundstrom and Rundqvist, 1965, p. 60)	11-13
Figure 5. Crystal structure of $\text{Mg}_2\text{Si}$ (Nowotny, Parthe and Lux, 1955, p. 866)	11-13
Figure 6. $\text{CuAl}_2$ structure projected on the basal plane. The black circles represent the silicon atoms (Aronsson, Lundstrom and Rundqvist, 1965, p. 60)	11-13
Figure 7. Crystal structure of $\text{Ta}_2\text{Si}$ of the $\text{CuAl}_2$ type (Nowotny, Parthe and Lux, 1955, p. 866)	11-13
Figure 8. The crystal structure of $\text{W}_5\text{Si}_3$ . Plane layers of atoms are connected by full or broken lines. The small circles represent the silicon atoms	17-18
Figure 9. Crystal structure of $\text{Ta}_5\text{Si}_3$ of the $\text{W}_5\text{Si}_3$ type	17-18
Figure 10. Crystal structure of $\text{Mn}_5\text{Si}_3$ . The small circles represent the silicon atoms. X shows the position of an octahedral void	17-18
Figure 11. Crystal structure of $\text{Ta}_5\text{Si}_3$ of the $\text{Mn}_5\text{Si}_3$ type	17-18
Figure 12. Hexagonal unit of the crystal structure of $\text{Mn}_5\text{Si}_3$	17-18

Figure 13. Apparatus for the hydrolytic reaction of the rare earth silicides	33
Figure 14. Sample tube	35
Figure 15. Gas sampling valve	39
Figure 16. Microscopic structure of dysprosium	48
Figure 17. Microscopic structure of $\text{Dy}_5\text{Si}_3$	49
Figure 18. Microscopic structure of erbium	50
Figure 19. Microscopic structure of $\text{Er}_5\text{Si}_3$	51
Figure 20. Microscopic structure of $\text{Ce}_5\text{Si}_3$ before it was annealed	52
Figure 21. Microscopic structure of $\text{Ce}_5\text{Si}_3$ annealed at $1000^\circ\text{C}$ for two hours	53
Figure 22. Microscopic structure of $\text{La}_5\text{Si}_3$	54
Figure 23. Microscopic structure of $\text{Pr}_5\text{Si}_3$ annealed at $1100^\circ\text{C}$ for two hours	55
Figure 24. Microscopic structure of $\text{Gd}_5\text{Si}_3$	56
Figure 25. Microscopic structure of $\text{Nd}_5\text{Si}_3$	57
Figure 26. Mass spectra of mono-, di- and trisilane	58
Figure 27. Mass spectra of tetra- and pentasilane	60
Figure 28. Relative molar response of n-paraffins and silanes versus molecular weight	71

## LIST OF TABLES

	page
Table 1. Products from the hydrolytic reactions of rare earth dicarbides.	24a
Table 2. The hydrolysis products from reactions of rare earth sesquicarbides with 1.0 n HCl.	26
Table 3. The retention times for the silanes. Flow rate of helium was 80 ml/min. The temperature of the gas chromatograph column was 65°C.	66
Table 4. Relative molar response for monosilane.	68
Table 5. Relative molar response for disilane.	69
Table 6. Results for the hydrolysis of rare earth silicides with 6 N $H_3PO_4$ .	72
Table 7. Hydrolytic reactions of $Ce_5Si_3$ with change in acid concentration ( $H_3PO_4$ ).	73
Table 8. Thermal conductivities and RMR for straight chained hydrocarbons and silanes at 300°K	78



## INTRODUCTION

The salt-like carbides, mainly the carbides of the alkali and alkaline earth metals, are non-conductors of heat and electricity, are chemically unstable and are readily decomposed by reacting with water vapor. Their chemical bonds have more ionic character than the refractory carbides.

In contrast, the refractory carbides, like the transition metal carbides, are very hard, are good conductors and are extremely stable chemically. The nature of their chemical bonds is complicated. Their high melting points and great hardness indicate covalent molecules similar to those in diamond while metallic bonds are suggested by their conductivity properties.

The carbides of the rare earth metals have physical properties similar to the refractory compounds; yet, like the salt-like carbides, they are readily hydrolyzed by water and generate hydrocarbons. In fact, the hydrolysis of the rare earth carbides have been studied extensively. The arrangement of the carbon atoms in the crystalline structure of these carbides and the degree of hybridization of the carbon orbitals for bonding in the crystals have been supported by the kinds and amounts of gaseous products from these reactions.

From the small amount of data available, the characteristics of silicides appear to be similar to the salt-like and

refractory carbides. Little information exists concerning the properties of the rare earth silicides. Their physical properties appear to be similar to the rare earth carbides. The purpose of this research was first of all, to observe whether or not the rare earth silicides of the general formula  $M_5Si_3$  would hydrolyze like the rare earth carbides and, secondly, to observe the kinds and amounts of the reaction products. In addition, the relative molar responses of monosilane and disilane in a gas chromatograph were measured and that of trisilane was obtained by extrapolation.

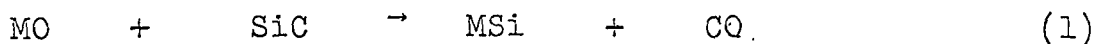
## LITERATURE REVIEW

## Rare Earth Silicides

In 1857, Deville and Caron prepared silicides of the alkali and alkaline earth metals and copper by reactions which were similar to those used in the preparation of the carbides. Even so, little attention was given to the chemistry and the preparation of these compounds until Moissan and Smiles (1902) investigated their formation in an electric furnace. In most of their preparations these men formed the silicides by the direct combination of the elements. Due to the nature of their apparatus and their experimental procedure, their compounds contained several phases. Nevertheless, improvements in their methods have now made direct combination of the elements the usual method of preparation. Because initiation of the reaction required high temperatures, it was necessary to exclude air in order to prevent oxidation of the silicides. The reaction could not be carried out in vacua since the volatilization of silicon prevented the production of stoichiometric compounds. This problem was solved by performing the reaction under a protective atmosphere of argon (Samsonov, 1959). Although contamination by oxygen was eliminated in this method, impurities were still prevalent from the materials of the crucibles which held the samples. Therefore, Samsonov and Neshpor (1960) prepared briquettes

from a powdered mixture of silicon and metal. The briquettes were sintered in a quartz tube in an argon atmosphere. They also tried hot pressing the powdered mixtures under a pressure of  $250 \text{ kg/cm}^2$  at  $1300\text{-}2150^\circ\text{C}$ . The latter method required repetitive treatment in order to avoid porosity. Another successful method for the direct union of silicon and a metal is the heating of appropriate mixtures in an arc furnace filled with an inert gas (Elektroschmelzwerk Kempton, 1963). Other methods for the preparation of silicides are briefly discussed in the following paragraphs.

(a) The thermal reduction of a mixture of a metallic oxide and silicon dioxide (or metal silicate) by carbon produces a metallic silicide (Elektroschmelzwerk Kempton, 1959; Samsonov, 1960). Two reactions are suggested for the reduction (Samsonov, 1960). They are:



(b) The reduction of a metal oxide by silicon yields a silicide according to the reaction



(c) The Goldschmidt thermite reaction produces silicides. This involves the reduction of a siliceous compound by powdered aluminum or magnesium in the presence of a free metal or metal oxide. (Samsonov, 1959)

(d) Silicides formed by the reaction of a metal halide with silicon or by the action of a silicon halide on a metal

(Latva, 1962).

(e) Reactions in molten alloys yield silicides as in the case of the dissolution of a metal in copper silicide.

(f) Silicides form during the high temperature electrolysis of molten salt baths containing a metal oxide and alkali fluosilicate (Hsu, 1961, Stern, 1960, Andrieux, 1938).

Usually, silicides form well shaped crystals which are brittle and hard. Their melting points and work functions are high. As a rule, they have a metallic luster which varies from silvery-white to gray. Most silicides which contain more than 50 percent metal show metallic conductivity. They have structures which range from typical alloy structures to the essentially salt-like compounds of the more electropositive elements. The chemical and physical properties of the silicides can be generalized for the two types of structures.

Salt-like silicides, particularly those formed by the alkali and alkaline earth metals, in contrast to alloy-type, refractory silicides,

(a) have relatively lower melting points and less thermal stability,

(b) have in general poorer thermal and electrical conductivity,

(c) have chemical bonds which are polar,

(d) are unstable, even in normally moist air, and

(e) are not resistant to air oxidation.

The refractory silicides are mainly compounds of the transition metal elements and silicon. The physical properties of these compounds are discussed by Aronsson (1965). He has also made the following comparisons of the metal silicides with the respective metal carbides, borides and nitrides;

(a) The silicides are easily cleaved whereas the carbides, nitrides and borides are not.

(b) The transition metal silicides have lower melting points, lower hardness, higher brittleness and lower creep strength in the hot condition than carbides, borides and nitrides.

(c) Silicides have a higher work function than carbides or borides.

(d) A decrease in the heat of formation (stability) with increasing transition metal group number is demonstrated by silicides, carbides, borides, nitrides and phosphides.

(e) The silicides, carbides, borides, nitrides and phosphides of the Group I through III (a) metals, including those of the lanthanides and actinides, are relatively unstable compounds which are easily decomposed by water, while those of the transition metals are refractory and chemically inert.

Silicon displays an appreciable solubility in some metals, particularly manganese, iron, cobalt and nickel. This phenomenon is explained by the fact that silicon can be easily accommodated in metallic structures by substitution in contrast to oxygen and nitrogen which dissolve interstitially in many

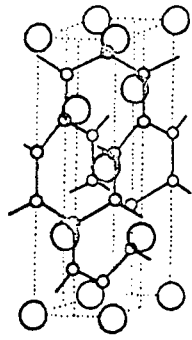
metals. The crystal structure of silicides takes varied forms and generalizations are not easily made for each group or family of elements. Those containing less than 33 percent silicon form mainly alloy-like, body-centered cubic or face-centered cubic structures. The disilicides,  $MSi_2$ , or those which contain 51-75 percent silicon generally have structures similar to  $AlB_2$ ,  $ThSi_2$  and  $GdSi_2$  types which are shown in Figures 1 and 2. (The  $GdSi_2$  structure is not shown in the figure since its structure is essentially a distorted  $ThSi_2$  type.) The rare earth disilicides are usually of the  $ThSi_2$  or  $GdSi_2$  types while some of the latter metals in the lanthanide series form silicides with the  $AlB_2$  structure. The silicides containing 33-50 atom percent silicon, some with the formula  $M_2Si$  have an anti- $CaF_2$  structure (see Figure 5). Other silicides containing similar amounts of silicon form structures of the type similar to  $CuAl_2$ ,  $U_3Si_2$ ,  $W_5Si_3$  and  $Mn_5Si_3$ .

The structure of  $CuAl_2$  is conveniently described as being built up of layers of metal atoms (A-layers) as shown in Figure 3. A single atom in a layer has eleven close neighbors. Successive A-layers are translated by half of the base diagonal to neighboring layers. Aluminum atoms fill the anti-prismatic holes between A-layers (see Figures 6 and 7).

In the  $U_3Si_2$  structure, successive A-layers are placed directly above one another to form the sequence A-A-A-... Silicon atoms fill the triangular prismatic holes and metal atoms fill the cubic holes between layers (see Figure 4).

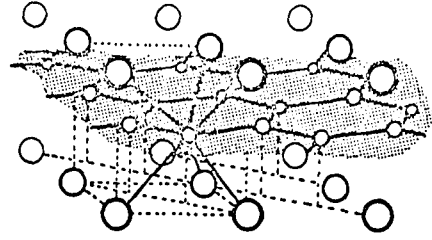
- Figure 1. The crystal structure of  $\text{ThSi}_2$  (Wells, 1962 p. 822)
- Figure 2. The crystal structure of  $\text{AlB}_2$ . The smaller circles represent B atoms (Wells, 1962, p. 774)
- Figure 3. A-layer of metal atoms (Aronsson, Lundstrom and Rundqvist, 1965, p. 60)
- Figure 4.  $\text{U}_3\text{Si}_2$  structure projected on the basal plane. The large circles represent the silicon atoms (Aronsson, Lundstrom and Rundqvist, 1965, p. 60)
- Figure 5. Crystal structure of  $\text{Mg}_2\text{Si}$  (Nowotny, Parthe and Lux, 1955, p. 866)
- Figure 6.  $\text{CuAl}_2$  structure projected on the basal plane. The black circles represent the silicon atoms (Aronsson, Lundstrom and Rundqvist, 1965, p. 60)
- Figure 7. Crystal structure of  $\text{Ta}_2\text{Si}$  of the  $\text{CuAl}_2$  type (Nowotny, Parthe and Lux, 1955, p. 866)



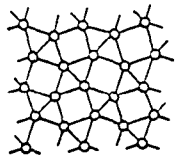


○ Th  
● Si

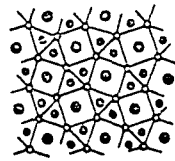
1



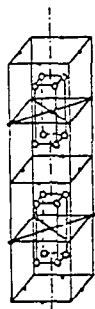
2



3

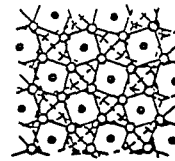


4

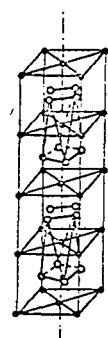


○ Mg  
● Si

5



6



○ Ta (Al)  
● Si (Cu)

7

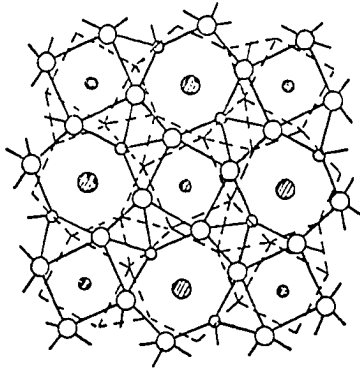
Similar layers which consist of metal and silicon atoms can be used to describe the  $W_5Si_3$  structure. For convenience, these layers are labeled B-layers (see Figures 8 and 9). In  $W_5Si_3$ , the sequence for the B-layers is denoted as B-B<sub>1/2</sub> 1/2 B-B<sub>1/2</sub> 1/2-where B<sub>1/2</sub> designates a B-layer translated by half of the base diagonal to neighboring layers. The square antiprismatic holes between B-layers in  $W_5Si_3$  are filled with metal atoms.

The  $Mn_5Si_3$  structure (see Figures 10, 11 and 12), commonly known as the Nowotny-phase, is composed of layers similar to  $W_5Si_3$  except the octahedral voids are not filled. Rare earth silicides of the formula,  $M_5Si_3$ , have this structure (Gladyshvskii, 1963). Because the silicon atoms in these structures are well separated by the metal atoms, one would predict the main product of hydrolysis to be monosilane.

#### Silanes

The simplest compound of silicon and hydrogen,  $SiH_4$ , was discovered by Buff and Wohler (1857). The air-sensitive gas was observed first as one of the products of the action of hydrochloric acid on some impure aluminum silicide. Subsequently, Wohler (1858) made the gas by reacting manganese or magnesium silicide with acids. The silanes were not fully characterized, however, until Stock and Somieski (1919) developed vacuum techniques to handle the air-sensitive gases. They prepared the silanes by the hydrolytic action of a mineral acid on magnesium silicide. About one-fourth of the magnesium

- Figure 8. The crystal structure of  $W_5Si_3$ . Plane layers of atoms are connected by full or broken lines. The small circles represent the silicon atoms. (Aronsson, Lundstrom and Rundqvist, 1965, p. 61)
- Figure 9. Crystal structure of  $Ta_5Si_3$  of the  $W_5Si_3$  type (Nowotny, Parthe and Lux, 1955, p. 866)
- Figure 10. Crystal structure of  $Mn_5Si_3$ . The small circles represent the silicon atoms. X shows the position of an octahedral void (Aronsson, Lundstrom and Rundqvist, 1965, p. 62)
- Figure 11. Crystal structure of  $Ta_5Si_3$  of the  $Mn_5Si_3$  type (Nowotny, Parthe and Lux, 1955, p. 866)
- Figure 12. Hexagonal unit of the crystal structure of  $Mn_5Si_3$



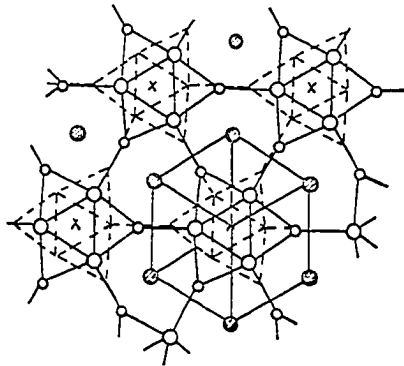
○ ○ ATOMS IN Z=0  
 ⊗ ○ ATOMS IN Z=1/4.314  
 --- ATOMS IN Z= 1/2

8



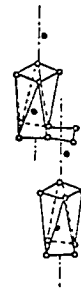
○ Ta  
 • Si

9



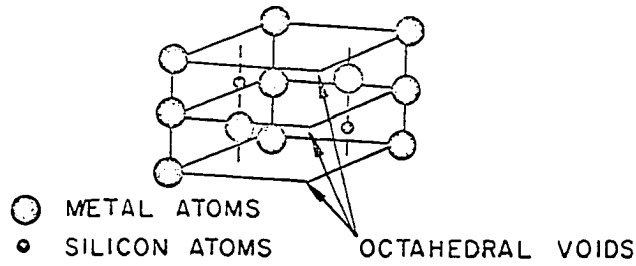
○ ○ ATOMS IN Z = 1/4  
 --- ATOMS IN Z = 3/4  
 ⊗ ○ ATOMS IN Z = 0.1/2

10



○ Ta  
 • Si

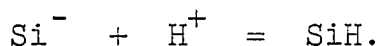
11



○ METAL ATOMS  
 • SILICON ATOMS  
 ○ OCTAHEDRAL VOIDS

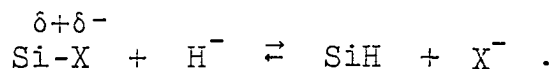
12

silicide was converted to mixtures of silicon hydrides. The mixture produced consisted of about 40 percent  $\text{SiH}_4$ , 30 percent  $\text{Si}_2\text{H}_6$ , 15 percent  $\text{Si}_3\text{H}_8$ , 10 percent  $\text{Si}_4\text{H}_{10}$  and 5 percent higher silanes. The mechanism of the hydrolysis was explained in terms of the attack of a proton on a negatively-polarized silicon atom according to the reaction



The hydrolytic action of hydrogen ions on silicides was observed in various solvent systems in an attempt to increase the yield of the products. The production of silanes was greater when magnesium silicide and ammonium bromide were reacted in either liquid ammonia (Johnson, 1935) or anhydrous hydrazine (Feher, 1955). The increase was attributed to the inertness of the silicon-hydrogen bond to ammonia.

The silanes were also prepared by the reaction between a metal hydride and a compound in which silicon was bound to a more electronegative element. Essentially, the process occurred between a positively polarized silicon atom and a hydride ion represented by the reaction



Lithium aluminum hydride dissolved in ether is the most commonly used source for hydride ions (Finholt, 1947). The higher silanes have also been prepared by passing silane through an ozonizer-type electric discharge (Gekhale, 1965).

Stock and Somieski (1916) established many of the physical properties of the silanes. They measured their melting and boiling points and found that monosilane and disilane were the only ones which were gaseous at room temperature. The chemistry of the SiH bond cannot be discussed accurately without considering the rest of the molecule to which it is bound. However, its chemical behavior can be predicted from a consideration of the dissociation bond energy and its role in similar reactions. The bond energy of Si-H is less than that of C-H. In contrast the bond energy between silicon and a more electronegative element, such as oxygen, is greater than that between carbon and a more electronegative element. Therefore, a Si-H bond in comparison with a C-H bond is more likely to react with an electronegative element in order to form a stronger bond. In other words, the Si-H bond is a stronger reducing agent. In addition, the Si-H bond requires less activation energy in order to initiate a reaction than C-H. This is particularly true when the silicon atom also forms a chemical bond with an electronegative atom. Reactions at the Si-H bond probably occur by the displacement of a hydride ion from the silicon atom. When this occurs, siliconium ions, analogous to carbonium ions, should form but they have not been observed experimentally in chemical reactions. The probable polarity of the Si-H bond accounts for its reactivity with Lewis acids (Ebsworth, 1963; Stone, 1962).

Monosilane reacts

(a) violently with oxygen, chlorine and bromine at room

temperature,

- (b) with iodine in the presence of aluminum iodide,
- (c) with HX in the presence of  $AlX_3$  (X = Cl, Br, and I),
- (d) with water in the presence of a base, and
- (e) with alcohols when it is catalyzed by a base, acid, silver ion or powdered copper.

Monosilane does not react

- (a) with nitrogen at 25°C,
- (b) with hydrocarbons at room temperature,
- (c) with ammonia except in the presence of amide ion, or
- (d) with pure water in quartz containers at room temperature.

Silicon hydrides react with Grignard reagents under certain conditions. They add across multiple carbon-carbon bonds when heated in the presence of peroxide or platinum metal catalysts. They reduce aqueous solutions of transition metal compounds. The fact that monosilane does not react with chloroform or carbon tetrachloride while the higher silanes react violently with them indicates that the SiH bonds are more reactive in the higher silanes.

The thermal stability of the silanes is less than that of the analogous paraffin hydrocarbons, and decreases with increasing molecular weight. Pure disilane decomposes slowly at room temperature. The decomposition rate increases with an increase in temperature or in the presence of monosilane (Harper, 1961).

Development of gas chromatography has made possible the separation and collection of longer chained silanes and their derivatives (Phillips, 1963). Squalane, tritolyl phosphate and silicone oil have been the most common liquid phases for the columns. Phillips, Timms, and Simpson (1964) separated heptasilane from the reaction products of the hydrolysis of magnesium silicide by gas chromatography and showed the presence of structural isomers of tetra and higher silanes.



## Hydrolysis of Rare Earth Carbides

The hydrolysis of rare earth carbides have been studied by Damiens (1913), Moissan (1920), Villehume (1951), Greenwood and Osborn (1961), Kanno and Kachi (1962), Palenik and Warf (1962), Svec, Capellen, and Saalfeld (1964), Pollard, Nickless, and Evered (1963), and recently Kosolapova, Kaminskaya, Kovalenko, and Pustovoit (1965). The results of these studies have not been the same for, seemingly, the same reactions. For instance, Damiens (1913) and Moissan (1920) did not observe the same amounts or kinds of gaseous products, except for ethyne, when they hydrolyzed the same rare earth dicarbides. Greenwood and Osborn reacted the rare earth dicarbides with sulfuric, nitric and chlorosulfuric acids as well as iodine. Although interesting, their results were obscured and complicated by various side reactions.

The results for the more recent experiments are summarized in Table 1. The quantity of hydrogen generated from the hydrolysis of  $\text{LaC}_2$  and  $\text{CeC}_2$  was not mentioned in the gas chromatograph experiments of Palenik and Warf (1962) and Kanno and Kachi (1962) since hydrogen was not collected in their work. Kosolopova et al. (1965) and Pollard et al. (1963) did collect hydrogen in their chromatography experiments. The work of Svec et al. (1964) was done by mass spectrometry techniques and therefore also permitted the observation and measurement of hydrogen. The following conclusions can be drawn from the table.

Table 1. Products from the hydrolytic reactions of rare earth dicarbides\*

Dicarbides	ethyne	ethane	ethene	methane	hydrogen	other products
Warf						
LaC <sub>2</sub>	A	B	C			
CeC <sub>2</sub>	A	B	C			
Kosolapova						
LaC <sub>2</sub>	A	D	C	B		
CeC <sub>2</sub>	A	C	D		B	
PrC <sub>2</sub>	A	B-C	D			B-C
NdC <sub>2</sub>	A	B-C	D			B-C
GdC <sub>2</sub>	A	D	C			B
Kanno						
LaC <sub>2</sub>	A	B	C			
CeC <sub>2</sub>	A	B	C			
Pollard						
LaC <sub>2</sub>	A	B	C		D	
CeC <sub>2</sub>	A	B	C		D	
NdC <sub>2</sub>	A	B	C		D	
GdC <sub>2</sub>	A	B	C		D	

\*The amounts of the products are labeled relative to one another for each reaction. The product with the largest yield is labeled A. The remaining products are labeled in the order of decreasing amounts, B, C, and D, respectively.

Table 1 cont'd.

Dicarbides	ethyne	ethane	ethene	methane	hydrogen	other products
Svec						
LaC <sub>2</sub>	A	C	D		B	
PrC <sub>2</sub>	A	D	C		B	
NdC <sub>2</sub>	A	D	B-C		B-C	
SmC <sub>2</sub>	A	D	C		B	
GdC <sub>2</sub>	A	D	B		C	
TbC <sub>2</sub>	A	D	B		C	
DyC <sub>2</sub>	A	D	C		B	
HoC <sub>2</sub>	A		C	D	B	
ErC <sub>2</sub>	A	D	C		B	
TmC <sub>2</sub>	A		D	C	B	
YbC <sub>2</sub>	A		C		B	D(1-Butyne)
LuC <sub>2</sub>	A			D	B	C(1-Propyne)

(a) The major product in all of the hydrolysis reactions is ethyne.

(b) With the exclusion of hydrogen (which is discussed later), the major products at room temperature from the hydrolysis of  $\text{LaC}_2$  and  $\text{CeC}_2$  are, in order of decreasing amounts, ethyne, ethane and ethene. Kosolapova et al. (1965) report a large amount of methane from the hydrolysis of  $\text{LaC}_2$ .

(c) In general, Kosolapova et al. (1965) and Svec et al. (1964) report hydrogen next in abundance to the production of ethyne. Pollard et al. (1963) disagree. They observed a relatively lower yield of hydrogen in comparison to the amounts of ethyne, ethane, and ethene. This difference has been attributed to the fact that their reactions were carried out at  $100^\circ\text{C}$  which promoted more hydrogenation of ethene and resulted in a greater amount of ethane and a decrease in hydrogen.

(d) With the exception of  $\text{YbC}_2$ , the hydrolysis of the heavier dicarbides beginning with  $\text{HoC}_2$  produces methane.

(e) Pollard et al. (1963) and Svec et al. (1964) report the appearance of 1-butene, 1,2-butadiene, and 2-butyne among the reaction products of the hydrolysis reactions.

Svec et al. (1964) hydrolyzed the rare earth sesquicarbides with 1.0 N HCl. (Pollard et al. reported data for the hydrolysis of  $\text{Y}_2\text{C}_3$  which agreed with Svec et al.) The results are recorded in Table 2. The conclusions which can be drawn from these results are listed below.

Table 2. The hydrolysis products from reactions of rare earth sesquicarbides with 1.0 N HCl<sup>a</sup>

Carbide	hydrogen	methane	ethene	ethane	ethyne	other
La <sub>2</sub> C <sub>3</sub>	A			C	B	D(butyne)
Ce <sub>2</sub> C <sub>3</sub>	B			C	A	D(butyne)
Pr <sub>2</sub> C <sub>3</sub>	B			C	A	D(butyne)
Nd <sub>2</sub> C <sub>3</sub>	B		D	C	A	
Sm <sub>2</sub> C <sub>3</sub>	A		D		B	C(butyne)
Gd <sub>2</sub> C <sub>3</sub>	B			C-D	A	C-D(butyne)
Tb <sub>2</sub> C <sub>3</sub>	A		C	D	B	
Ho <sub>2</sub> C <sub>3</sub>	B	D	C		A	
Er <sub>2</sub> C <sub>3</sub>	A	C		D	B	
Tm <sub>2</sub> C <sub>3</sub>	C	B			D	A(propyne)
Lu <sub>2</sub> C <sub>3</sub>	C	A			D	B(propyne)
Y <sub>2</sub> C <sub>3</sub>	B	C	D		A	

<sup>a</sup>The amounts of the products are labeled relative to one another for each reaction. The products are labeled in order of decreasing amounts, A, B, C, and D, respectively.

(a) Lighter metal carbides produce more butyne.

(b) Acetylene is the major product from the lighter carbides.

(c) Heavier carbides show a greater production of methane and propyne.

The hydrolysis of the rare earth sesquicarbides produces more methane and propyne than the hydrolysis of the rare earth dicarbides under the same reaction conditions. The larger production of odd numbered hydrocarbons has been attributed to the existence of  $C_3^{-4}$  groups in the crystal structure of the sesquicarbides (Kanno and Kachi, 1962). This cannot be taken seriously since crystallography studies have shown that  $C_2^{-2}$  groups occur in the crystal structure for  $Y_2C_3$  (Atoji et al., 1958).

Palenik and Warf (1962) have reported no ethyne and more odd numbered hydrocarbons when the dicarbides are hydrolyzed at a high temperature. Moissan (1920) found no difference in the reaction products when the hydrolyses were performed at  $0^\circ C$  and room temperature.

If the strength of the acid used as the hydrolyzing reagent is varied, the relative amounts of the products varies accordingly (Svec et al. 1964; Pollard et al. 1963). No difference is observed in the relative amounts of products when the hydrolyzing agent is  $H_2O$ ,  $HCl$ , or  $H_2SO_4$ , although the latter does give higher yields (Pollard et al. 1963). Nitric acid, on the other hand, curtails hydrogenation and

polymerization since it produces less ethane, acetylene, C<sub>4</sub>-hydrocarbons and more ethylene. The free radical reactions



are well known (Forsyth, 1941). Perhaps these reactions prevent the recombination of radical fragments to form longer chains.

## EXPERIMENTAL PROCEDURES

## Preparation of the Rare Earth Silicides

Lanthanum, cerium, praseodymium, neodymium, gadolinium, dysprosium and erbium were obtained in the form of rods,  $3/8$  inches in diameter, from the Ames Laboratory of the A.E.C., Ames, Iowa. When the metals were obtained from the laboratory, their maximum purity was approximately 99.5 percent by weight. The impurities on an atom percent basis were mainly interstitial elements such as oxygen, nitrogen and hydrogen. A portion of the rods was machined in a small lathe mounted in a controlled atmosphere box. The box was continuously flushed with helium during the machining of the metal. The machined metal rod was placed in a vial which was previously flushed with helium. The metal was delivered in this form to the arc melter for the combination with silicon.

The rare earth silicides,  $M_5Si_3$ , were prepared under one atmosphere argon in a nonconsumable arc furnace. A water cooled tungsten electrode was used as the cathode and a water-cooled copper hearth, the anode, was used as the mold in order to eliminate crucible contamination during the melting. Stoichiometric amounts of silicon (c. 0.5 grams) and rare earth metal (c. 4.5 grams) were weighted exactly and placed in a dish-shaped indentation or mold in the copper hearth. The reaction chamber was evacuated to a pressure of  $10^{-2}$  to  $10^{-3}$  torr before it was filled with tank argon to one atmosphere



pressure. The samples were melted by an arc from the tungsten electrode operated at 30 volts DC with 100-150 amperes of current. Prior to the melting of any samples, a zirconium getter button was melted several times in order to purify the argon of residual nitrogen and oxygen. Each melted sample was turned upside down and remelted. This process was repeated several times in order to achieve maximum homogeneity and to insure complete reaction in the center of the specimen. Each rare earth silicide button prepared was embedded in Bakelite and cut so that a section of the silicide was exposed. The surface was mechanically polished on a Syntron vibratory polisher (Syntron Company, Homer City, Pa.) which had a hard wax polishing surface and a water suspension of alumina polishing compound. Photographs were taken on the polished surface at 250 x magnification by means of a Bausch and Lomb Research Metallograph. This was done in order to determine the purity and uniformity of the silicide. Also, for the same purpose powder patterns and diffractometer traces were made with a Debye-Scherrer X-ray apparatus.

#### Preparation of the Silanes

A diagram of the apparatus used for the preparation of the silanes and for the hydrolytic reactions of the silicides is given in Figure 13. Before the experimental conditions and procedures for the reactions are discussed, brief descriptions of some of the components of the apparatus follow.

The reaction vessel, shown in Figure 13, is a closed bottom

tube, 18 cm x 1.5 cm, with an enlarged open top. Near the enlarged portion leading from the reaction vessel is attached a side arm. A large bulb, 4.5 cm in diameter, is blown into the side arm in order to trap any liquid which boils from the reaction. The reaction vessel is of such size that a rubber, serum bottle septum fits snugly in the enlarged portion. During the reactions a pool of mercury covers the septum to insure that the reaction is completely isolated from the atmosphere.

The drying tubes, illustrated in Figure 13, were Pyrex brand glassware (Schwartz absorption tubes, Corning Glass Works, Corning, New York). Each tube was filled with phosphorus pentoxide in a dry box. The drying agent was held in both arms of the drying tube by means of glass wool.

The sample tubes, illustrated in Figure 14, were U-shaped. The distance between the arms of the U was approximately 4 cm and the length of the arms from the bottom of the U was approximately 14 cm. The bore of the tube was 6 mm in diameter. Each sample tube was filled with Celite Analytical Filter-Aid (Johns-Manville, 22 East 40th St., New York, New York) coated with 10 percent Silicone Oil 702 (Dow Corning Corp., Midland, Michigan, U.S.A.). The Celite was held in place by glass wool tucked into each arm of the U-tube. The top of each arm of the U-tube was fitted with a Teflon needle valve (1 mm, Lab-Crest, Fisher and Porter Co., Warminster, Pennsylvania) which screwed into a 1 mm glass constriction to form a seal. Connected perpendicularly

Figure 13. Apparatus for the hydrolytic reaction of the rare earth silicides

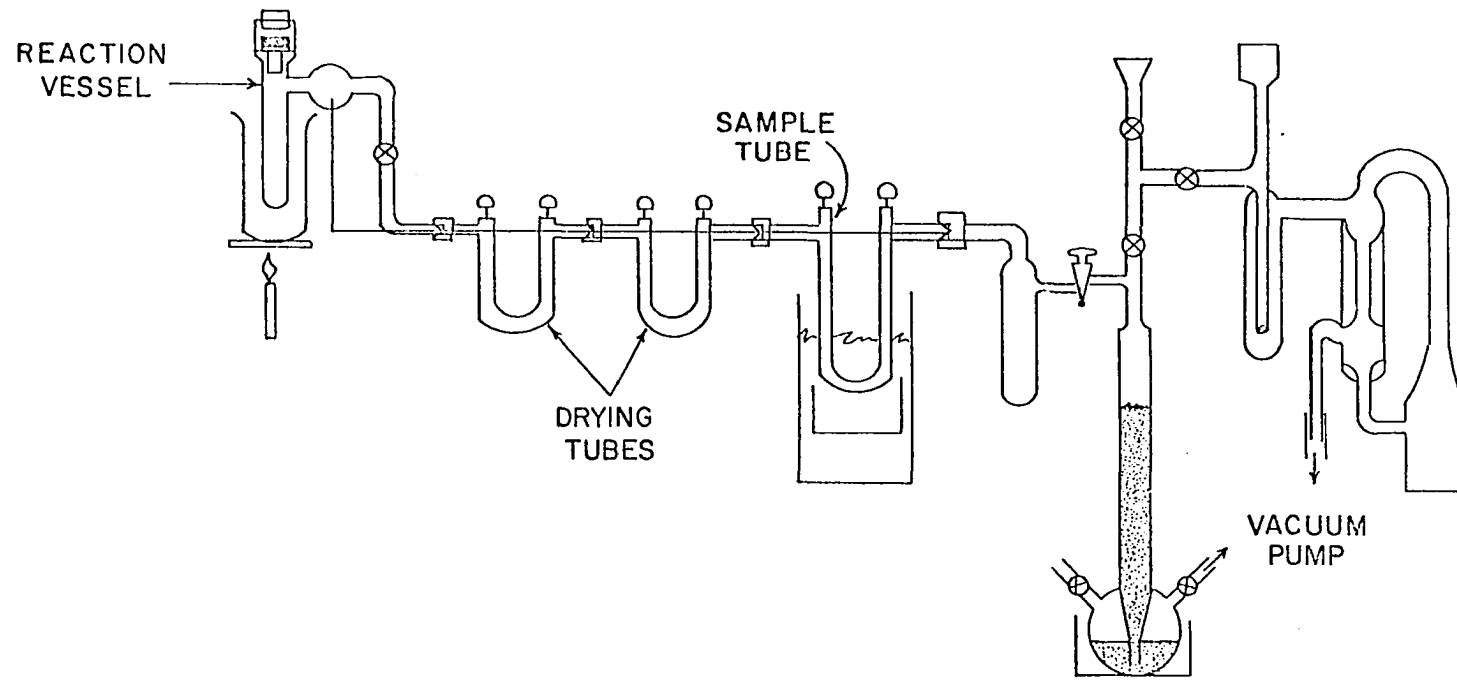
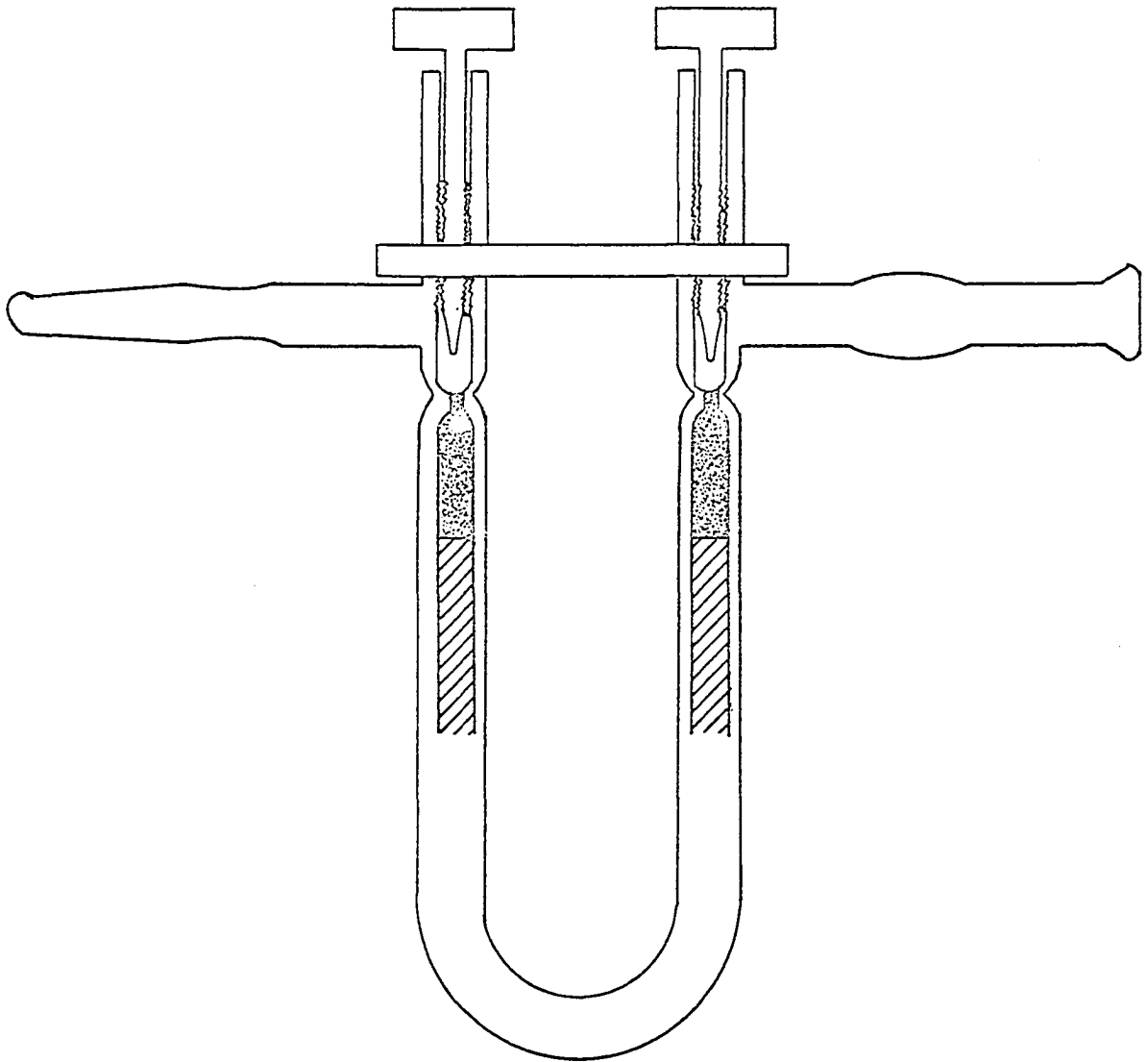


Figure 14. Sample tube



SAMPLE TUBE

to each of the needle valves and to each of the arms of the U-tube was an outer or inner 7/25 tapered glass joint.

The reaction vessel, two drying tubes, a sample U-tube, a diffusion pump and a mechanical pump were connected in sequence in that order. During the preparation of silanes for the purpose of identifying their peaks on the gas chromatograms, magnesium silicide was reacted with 20 percent  $H_3PO_4$ . The reaction vessel was thermostated in a beaker of boiling water in order to vaporize the higher silicon hydrides. Heating tapes (110 volt, 8' x 11", Bristheat, Briscoe Mfg. Company, Columbus, Ohio) were wrapped around the tubes connecting the reaction vessel, the drying tubes and the sample U-tube. The tape was operated at approximately  $100^\circ C$  in order to prevent the condensation of the higher silicon hydrides in the connective tubes. After the apparatus was assembled, magnesium silicide, previously pulverized in a steel mortar and pestle, was dropped into the reaction vessel and the entire system was evacuated. The serum bottle stopper was sucked into place and covered with mercury. When the pressure of the system became approximately  $10^{-3}$  torr as indicated by an ion gauge, the sample U-tube was cooled by raising a Dewar of liquid nitrogen around it. The reaction was started slowly at first by injecting a small amount of 20 percent phosphoric acid through the pool of mercury and the rubber septum by means of a syringe (B-D Yale Luer-Lok, Becton, Dickinson and Co.). The gaseous products were condensed and absorbed in the sample U-tube while

the non-condensables, such as hydrogen, were pumped away. After the reaction was complete, the valves on the sample U-tube, as well as the rest of the stopcocks in the system, were closed. The sample U-tube was removed and taken to the gas chromatograph inlet system. The same procedure was used for the reaction of the rare earth silicides. The duration of the hydrolytic reactions ranged from 2 to 4 hours. Approximately 150 mg. of the rare earth silicide required about 10 ml. of acid for complete hydrolysis.

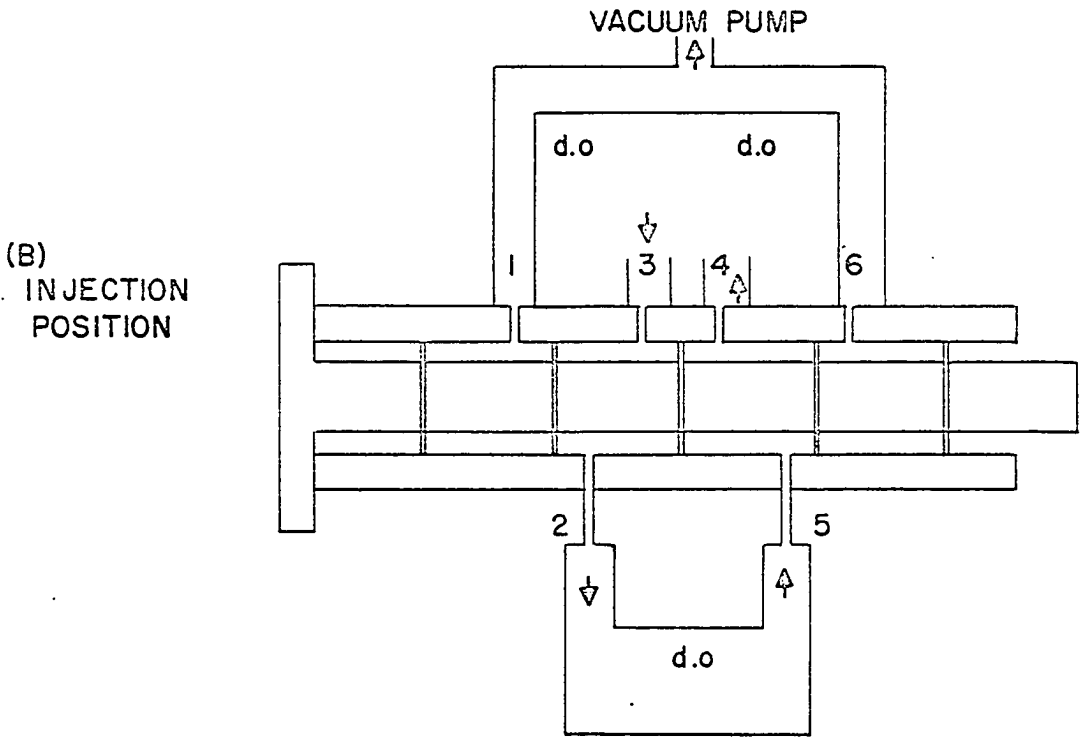
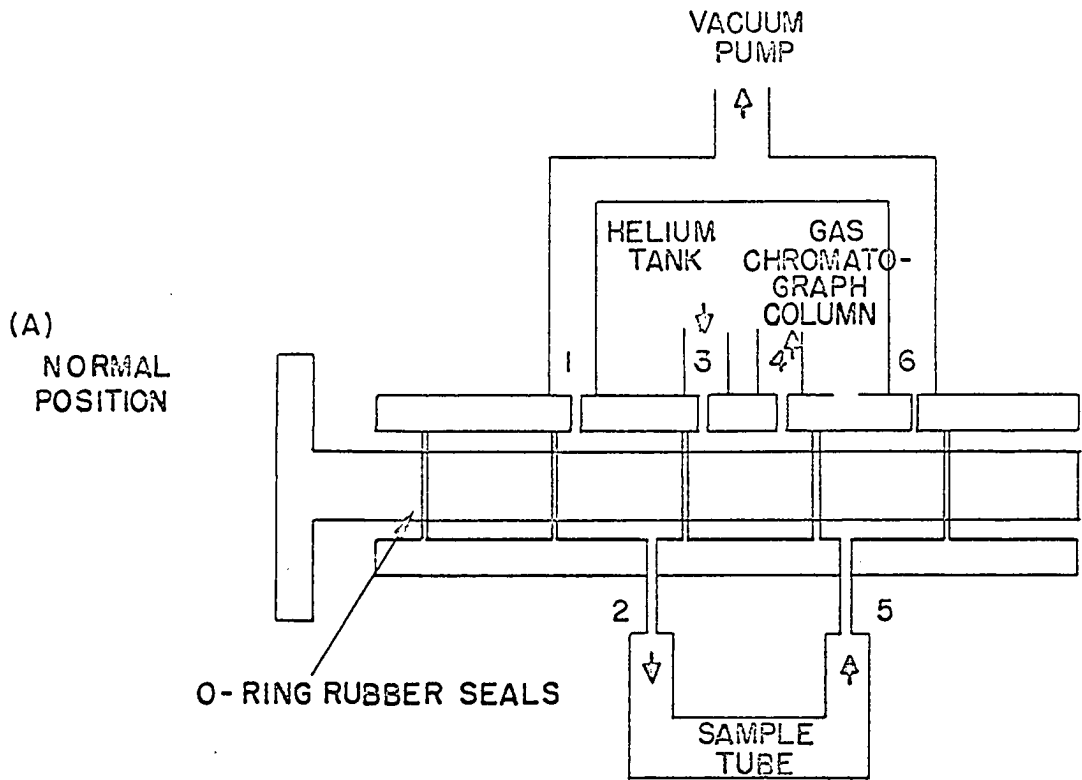
#### Separation and Identification of the Silanes

The apparatus used for the separation and collection of the silane fractions for identification can be divided into four parts: (a) the inlet system to the gas chromatograph, (b) the gas chromatograph, (c) the collection system, and (d) the mass spectrometer.

(a) The most important part of the inlet system is the gas sampling valve (XA-204, Wilkens Instrument and Research, Inc., Walnut Creek, California). A cross sectional diagram of the gas sampling valve is illustrated in Figure 15. Ports 1 and 6 are connected to a vacuum pump. Ports 3 and 4 are connected to the helium supply and the entrance of the chromatograph column, respectively. Ports 2 and 5 connected to the sample U-tube. When the plunger is pulled, helium flows into port 3 and exits through port 4. In this portion the sample U-tube and the vacuum pump are isolated from the flow of helium. This allows the space between the Teflon valve of the



Figure 15. Gas sampling valve



GAS SAMPLING VALVE

sample U-tube and the gas sampling valve to be evacuated before the air-sensitive silanes are flushed into the gas chromatograph. When the plunger is pushed, the helium is directed through ports 3 and 2 to one side of the sample U-tube, picks up the sample, and returns through the ports 5 and 4 of the gas sampling valve on its way to the chromatograph column. With the plunger in this position, the tubes leading to the vacuum pump are isolated from the flow of helium and the sample.

The copper tubing leading from the ports 2 and 5 are connected to an outer and inner 7/25 tapered glass joints, respectively, by means of Kovar seals. The sample U-tubes are fastened to the tapered glass joints by means of Apiezon W. Wax.

(b) The gas chromatograph (Autoprep Model A-700, Wilkens Instrument and Research, Inc., Walnut Creek, California) contains an aluminum column, 10' x 3/8", packed with 10 percent methyl silicone fluid (SF-96, Wilkens Instrument and Research, Inc., Walnut Creek, California) on Chromasorb T. A thermal conductivity cell made with tungsten filaments is used as a detector. The unit is designed with heaters within the housings for the column, the detector and the liquid sample injection port. Throughout the entire work with the silanes, the temperature for the sample inlet and detectors was kept at approximately 100°C. The sample tubes were also kept at ~100°C by means of a beaker of boiling water. The oven temperature for the column was maintained at 65°C by means of a

thermostat and an oven fan which continuously stirred the air around the column. The unit was equipped with a bubble flow meter for measuring the flow rate of helium through the column. The flow was timed with a Lab-Chron 1401 Timer (Labline, Inc., Chicago, Illinois). For the collection of longer chain silanes with large retention times, the flow rate was regulated at 80 ml/min; while for the identification of the products from the hydrolysis reactions of the rare earth silicides, it was set at 40 ml/min. In order to improve the resolution of the chromatogram peaks, a copper column, 8' x 3/8", packed with 10 percent Silicone Oil 702 (Dow Corning Corp., Midland, Michigan) on Celite Analytical Filter-Aid (Johns-Manville, 22 East 40th Street, New York, New York) was added.

Grade A helium (Bureau of Mines, Amarillo, Texas) which was double-filtered through activated charcoal by the supplier, was introduced into the column at a pressure of 50 p.s.i. The 7/25 tapered glass joints of the sample U-tubes were sealed to the tubes leading to the gas sampling valve with Apiezon W wax. The sample U-tubes were thermostated in boiling water and a heating tape (Briskeat, Briscoe Mfg. Company, Columbus, Ohio) was wrapped around the glass and copper tubing leading to the column. This was kept at approximately 100°C in order to prevent the condensation of the longer chain silicon hydrides. Before the introduction of each gas sample to the chromatograph, the air was pumped from the connective tubes between the sample U-tube and the gas sampling valve. This required approximately

thirty minutes. During this time the sample U-tube temperature was approaching 100°C. The plunger of the gas sampling valve was pushed and the valves to the sample U-tube were opened, permitting helium to flush the sample into the column.

(c) When a silane fraction emerged from the chromatograph as indicated by the formation of a peak on the chromatogram, a liquid nitrogen trap was raised around the collection U-tube which was previously flushed with helium. With the completion of the peak, the valve on the collection U-tube furthest from the chromatograph was closed, followed by closing the valve on the collection U-tube next to the chromatograph. This precaution was taken to prevent the back-influx of oxygen from the atmosphere. The collection U-tube was delivered to the mass spectrometer in order to identify the chromatograph peak or to a special manometer in order to measure the number of moles for the calculation of the relative molar responses of silane, disilane and trisilane.

(d) A 60° magnetic sector mass spectrometer (Sparrow, 1966) was used for the identification of the chromatogram peaks. The silane fractions were introduced into the mass spectrometer at a pressure of  $2 \times 10^{-5}$  torr and ionized with 70 eV bombarding electrons. Xenon was added with the silanes in order to aid the assignment of the masses of the ion peaks.

#### Relative molar responses

The determination of the relative molar responses required, in addition to the apparatus already mentioned for the

preparation of pure fractions of silanes, a manometer and a precise knowledge of the volume of the collection U-tubes. The manometer was of usual design made from 2 mm glass capillary. The collection U-tubes were calibrated for volume by weighing the tubes filled with mercury and calculating the volume from the density of mercury.

In the procedure for the determination of the relative molar response, the collection U-tube containing the condensed silane was taken from the chromatograph and attached directly to a vacuum line. The valves on the collection tube were closed while the air was pumped from the connecting tubes. The collection U-tube was cooled in liquid nitrogen. The valve of the collection U-tube leading to the vacuum pump was opened until the pump stopped "gurgling". The purpose for this was to pump the helium from the sample tube before pressure measurements were made of the collected silanes.

The collection U-tube was removed from the vacuum line and connected to the manometer. While the U-tube was approaching room temperature, the space between the mercury column and the collection U-tube was pumped for at least an hour. The valve leading to the vacuum pump was closed and the needle valve of the collection U-tube opened. The change in pressure readings was recorded. The needle valve was closed. The collection U-tube was removed and returned to the inlet system of the gas chromatograph. The previously mentioned procedure was used to introduce the silane again through the chromatograph

column. Two microliters of benzene was introduced along with the silane, through the injection port by means of a microliter syringe (705 N. Hamilton Company, Inc., Whittier, California). The benzene served as a standard reference for the determination of the relative molar response for the silanes. The relative molar responses for the hydrocarbons were similarly determined by Rosie and Grob (1957) and Messner, Rosie, and Argaright (1959). The areas of the peaks were measured with a compensating polar planimeter (K + E 4242 Keuffel and Esser Co., Germany).

## CALCULATIONS

The relative molar response (RMR) for mono- and disilane was calculated in the same manner as the relative molar responses for the hydrocarbons (Messner, Rosie and Argaright, 1959). The equation for the calculation is:

$$\frac{(\text{RMR of silane}) (\text{Moles of silane})}{\text{Area of silane peak}} = \frac{(\text{Moles of benzene}) (\text{RMR of benzene})}{\text{Area of benzene peak}} .$$

The RMR of benzene was arbitrarily chosen to be 100. The number of moles of silane was calculated from the gas law equation,  $PV = nRT$ , where

V = the volume of the collection U-tubes (6.5178 ml. and 5.9298 ml),

R = the gas constant (6236. ml-cm/deg-mole),

T = the absolute temperature ( $^{\circ}\text{K}$ ),

P = the change in pressure (cm) and

n = the number of moles.

The relative molar response for monosilane was determined before that of disilane. This was necessary for the calculation of the RMR for disilane since the chromatogram for the disilane decomposed to form monosilane or else the separation of the disilane fraction from the monosilane was not complete in the chromatograph. At any rate the number of moles of monosilane was calculated from the area of its chromatogram peaks and its



previously measured RMR and was subtracted from the total moles collected in the U-tube in order to ascertain the number of moles of disilane.

Later in the discussion, calculated values for the thermal conductivities of the silanes are given in Tables 5 and 6. These calculations are discussed in the Appendix.

## RESULTS

## Rare Earth Silicides

The microphotographs of the rare earth silicides are shown in Figures 17, 19 - 25. The black spots are probably cavities in the surface while the gray areas are most likely another phase. Since the diffractometer traces and the X-ray powder patterns revealed no strong indications of free metal or of free silicon, the gray areas are perhaps oxides, although the X-ray data do not indicate this. This phase is not concentrated enough to produce definitive X-ray identification. The small black areas in the picture for the respective silicides of the metals (see Figures 17 and 19), is an indication that the impurities might have volatilized in the formation of the silicides.

## Mass Spectra of Silanes

The mass spectra of the silanes obtained here are given in Figures 26 and 27 along with those reported by Pupezin and Zmbov (1958), Callery Chemical Co. (ca. 1950), and Svec and Saalfeld (1963).

Reactions for the silanes which are initiated by a bombarding electron must explain the following observations for the silane fragmentation patterns:

(1) A large ion peak was recorded at  $m/e = 120$  and at  $m/e = 60$  as long as pentasilane molecules were present in the source. The presence of pentasilane was followed by the occurrence of

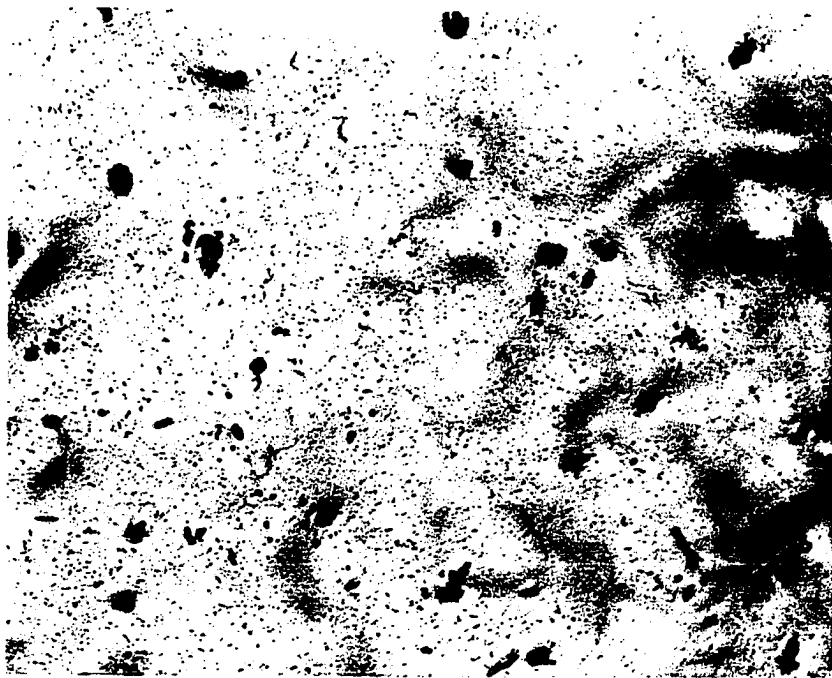


Figure 16. Microscopic structure of dysprosium

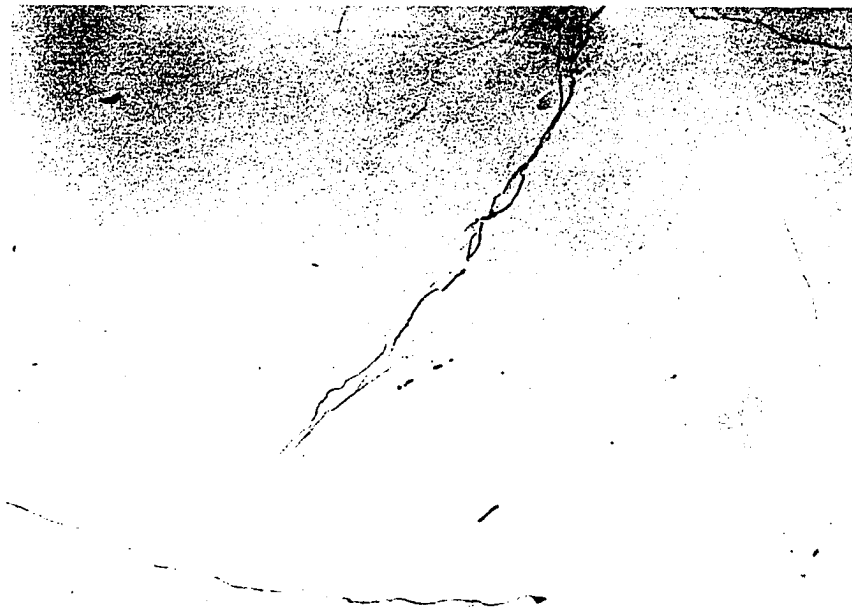


Figure 17. Microscopic structure of Dy<sub>5</sub>Si<sub>3</sub>

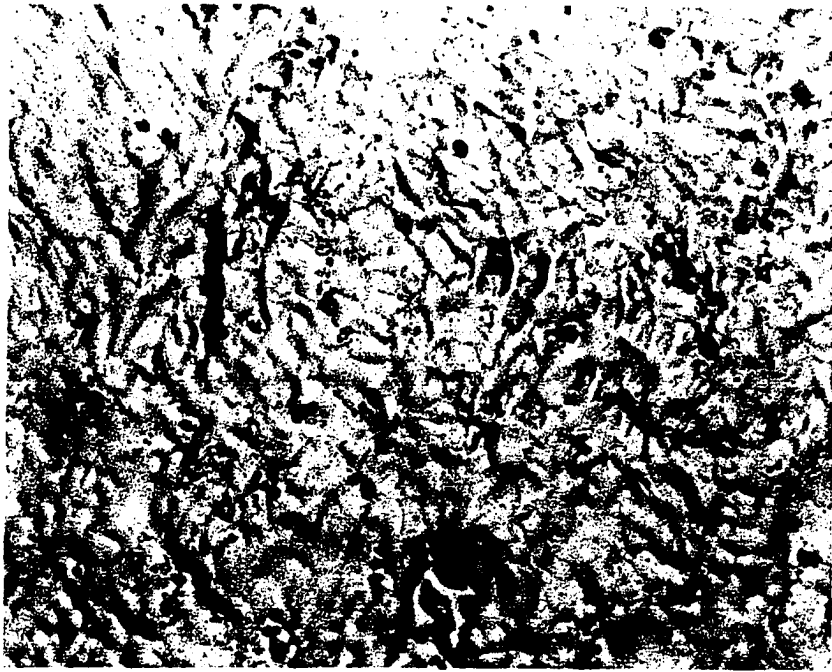


Figure 18. Microscopic structure of erbium

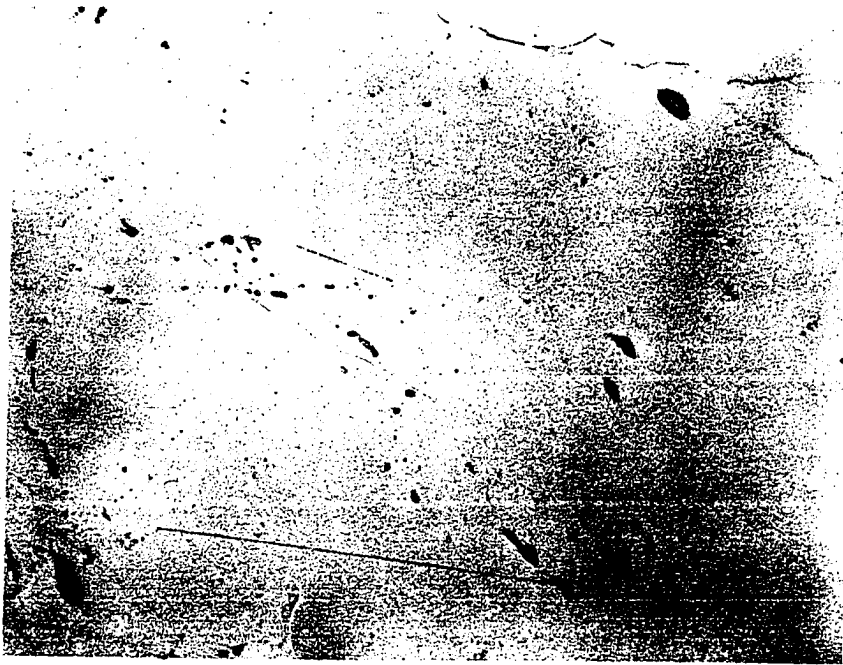


Figure 19. Microscopic structure of Er<sub>5</sub>Si<sub>3</sub>

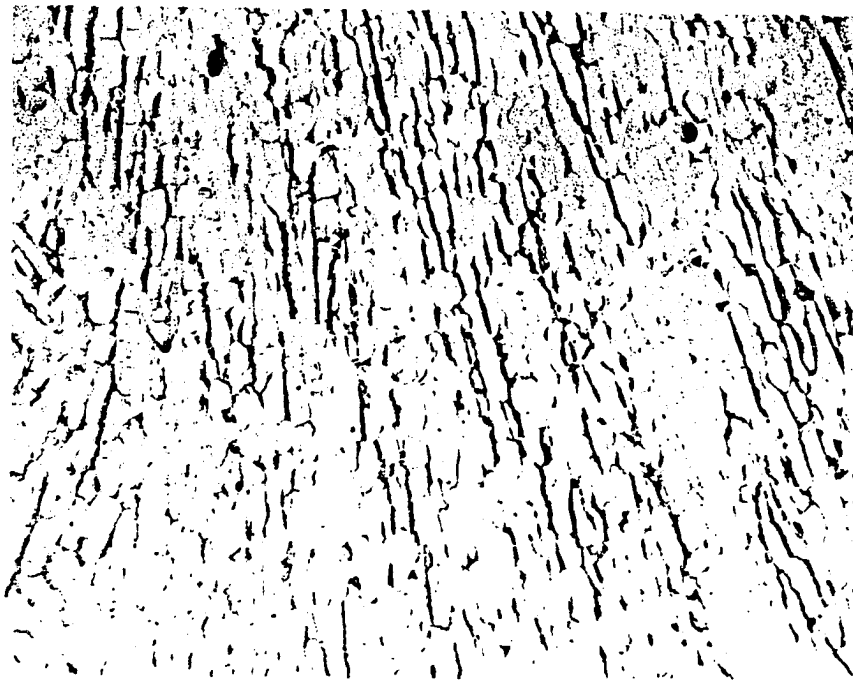


Figure 20. Microscopic structure of Ce<sub>5</sub>Si<sub>3</sub> before it was annealed

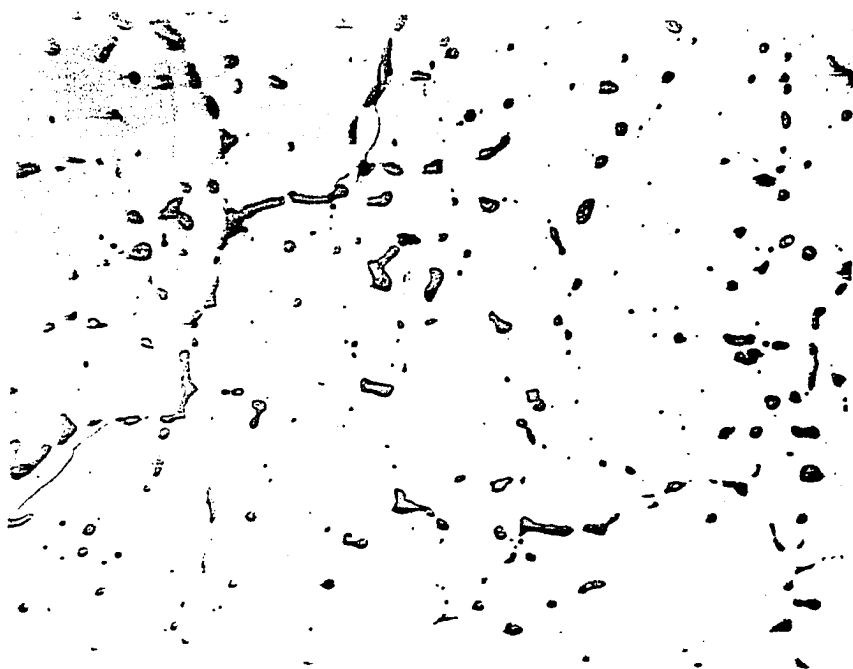


Figure 21. Microscopic structure of Ce<sub>5</sub>Si<sub>3</sub> annealed at 1000°C for two hours





Figure 22. Microscopic structure of  $\text{La}_5\text{Si}_3$

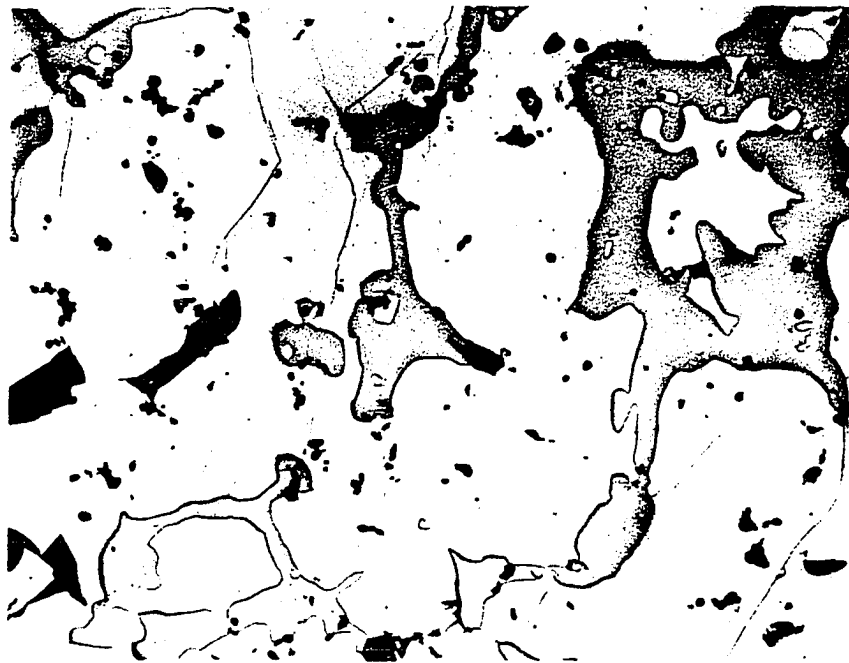


Figure 23. Microscopic structure of Pr<sub>5</sub>Si<sub>3</sub> annealed at 1100°C for two hours.

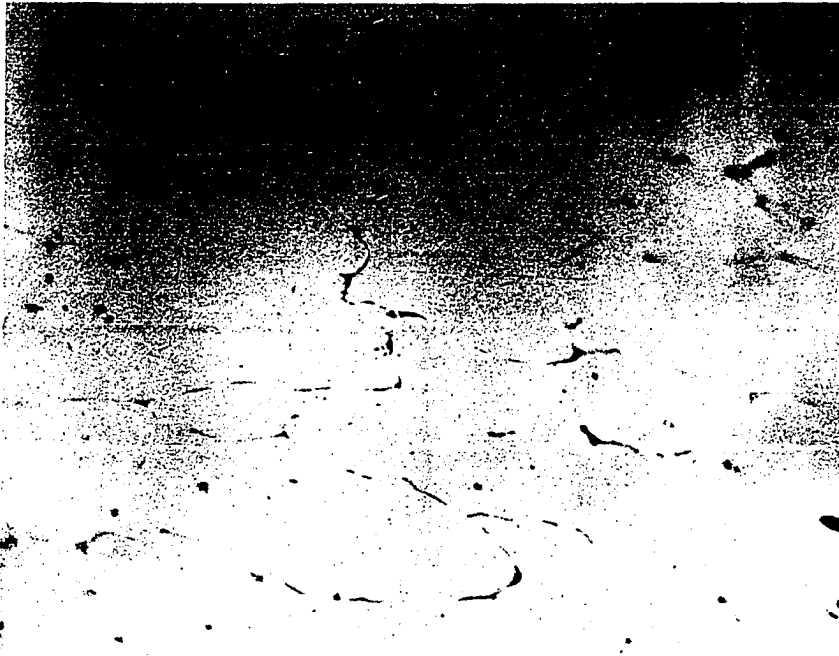


Figure 24. Microscopic structure of  $Gd_5Si_3$

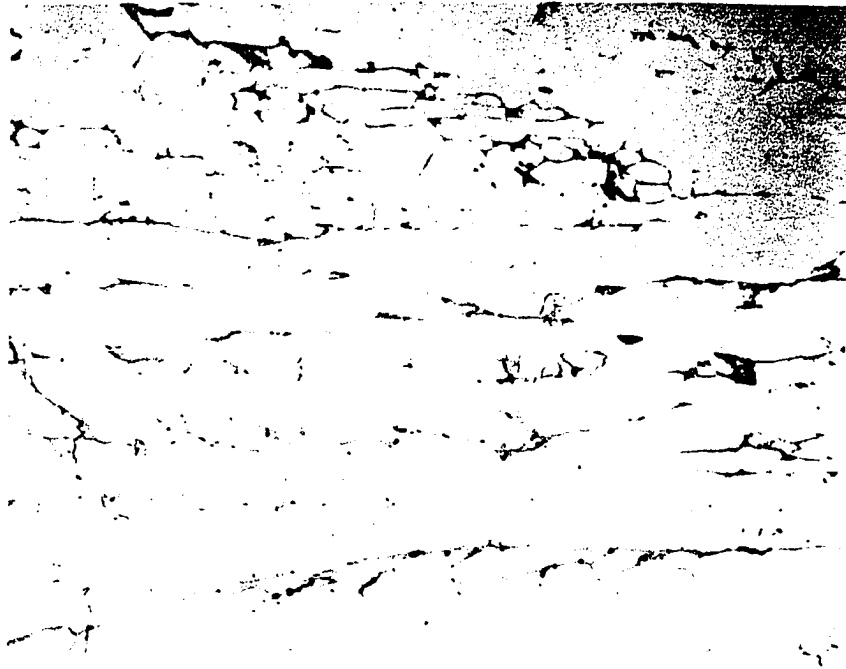


Figure 25. Microscopic structure of Nd<sub>5</sub>Si<sub>3</sub>

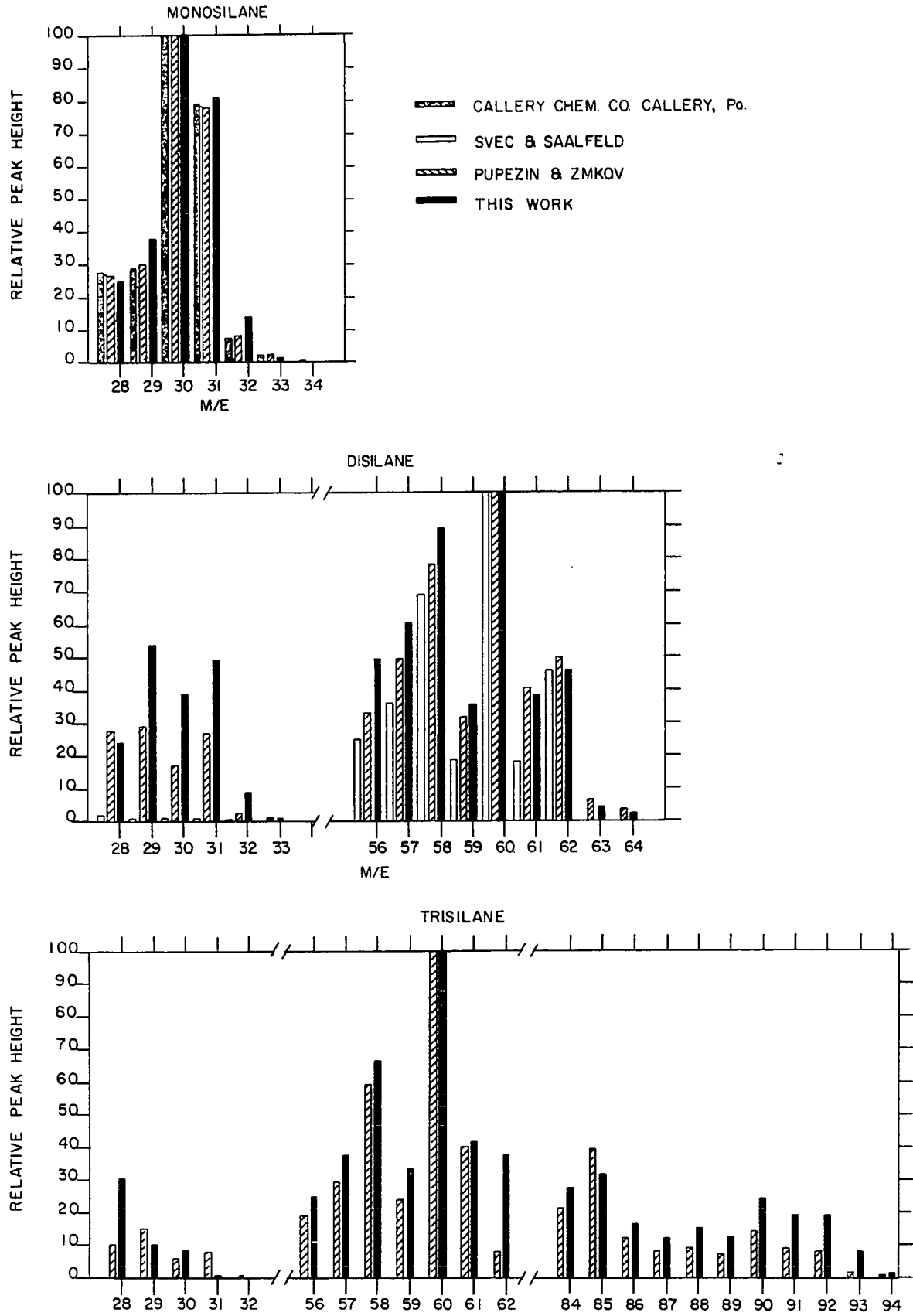
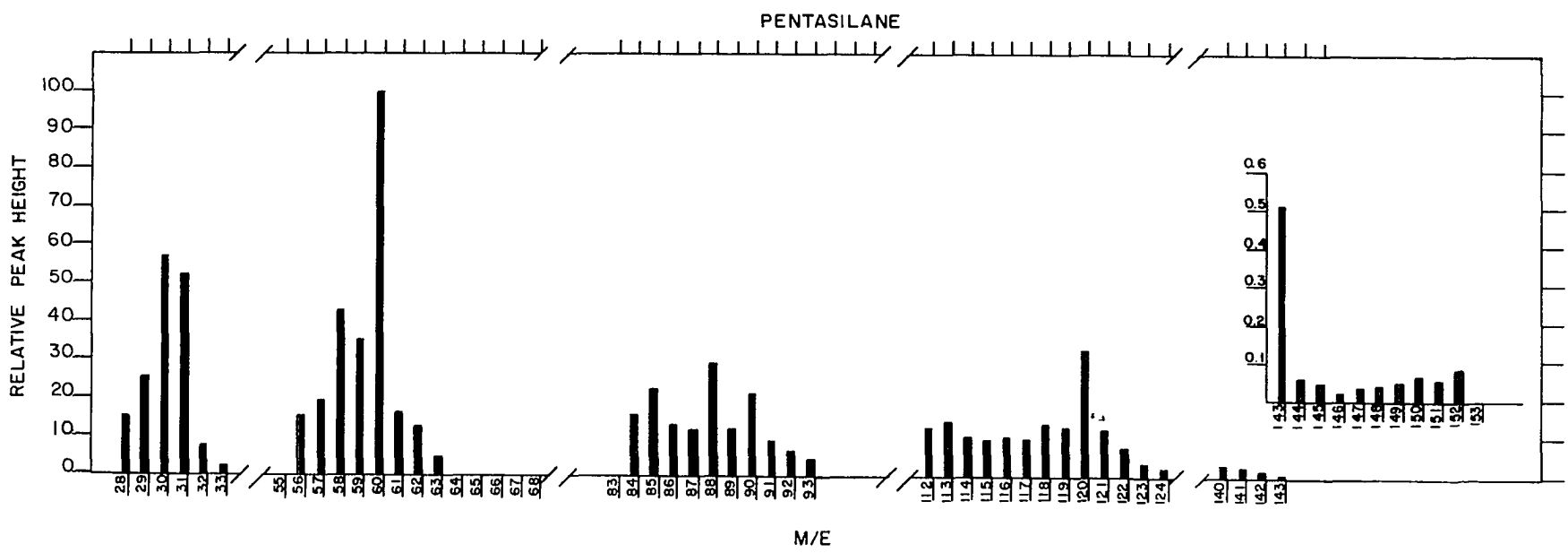
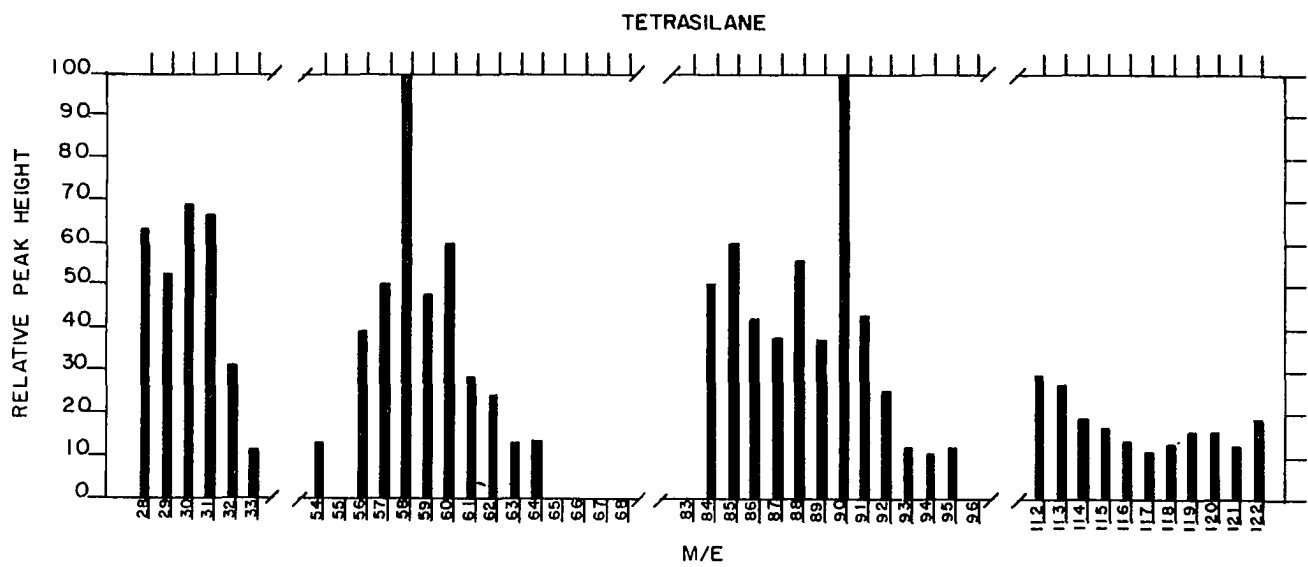


Figure 26. Mass spectra of mono-, di- and trisilane

Figure 27. Mass spectra of tetra- and pentasilane



the ion peaks at  $m/e = 140$  to  $m/e = 152$ .

(2) During the decomposition of pentasilane, the ion peak at  $m/e = 120$  became smaller as the ion peak at  $m/e = 90$  became larger.

(3) After the complete decomposition of pentasilane, the large ion peaks were at  $m/e = 58$  and at  $m/e = 90$ . This stage of the pentasilane spectrum corresponded to the tetrasilane spectrum.

(4) During the decomposition of tetrasilane, the ion peak at  $m/e = 90$  became smaller while the ion peak at  $m/e = 60$  became larger.

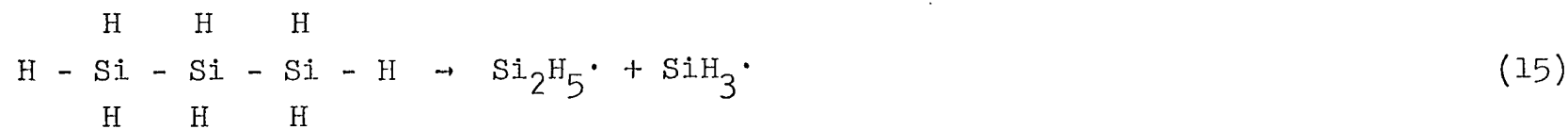
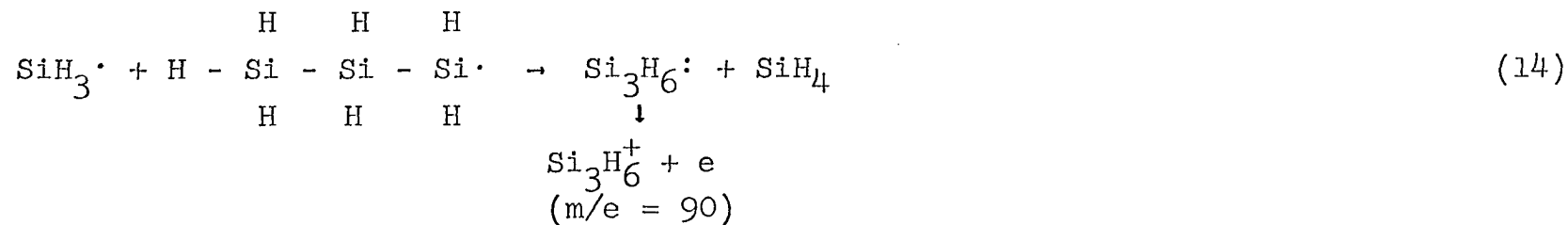
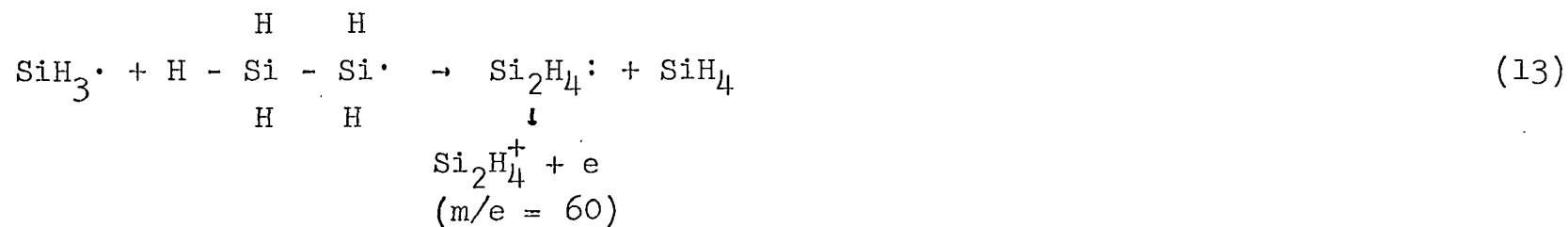
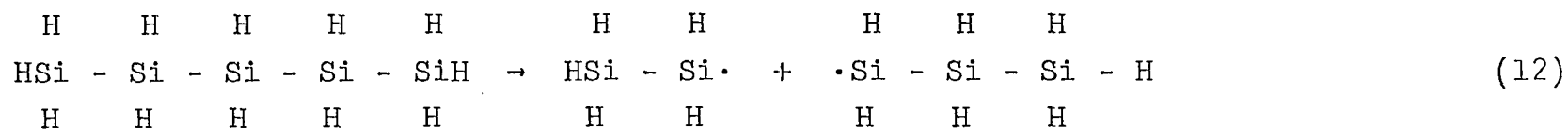
(5) After the complete decomposition of tetrasilane, the largest ion peak occurred at  $m/e = 60$ . This stage of the pentasilane or tetrasilane spectrum corresponded to the spectrum for trisilane.

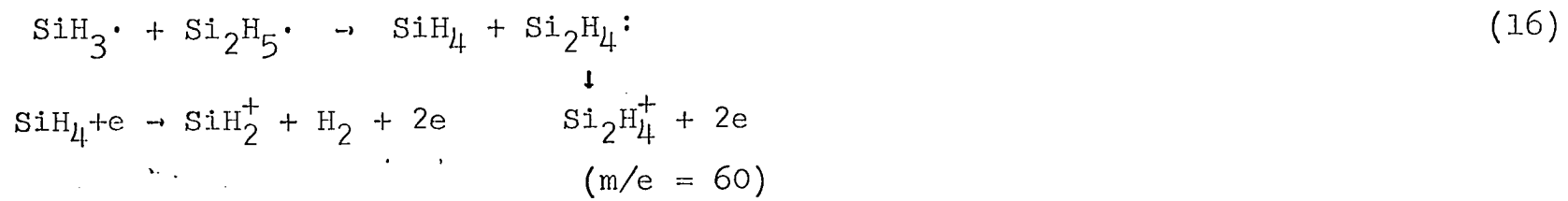
The bond-breaking and bond-forming processes which may be taking place are diagrammed in the equations on the following pages.

The energy for the Si-Si bond is approximately 25 kcal/mole less than the energy for the Si-H bond; (Ebsworth [1963]) hence, the splitting of the silyl radical from a pentasilane molecule (Equation 6) is more probable than the elimination of a hydrogen atom from the pentasilane molecule. Equation 7 is more probable than equation 8. The removal of a second hydrogen atom from monosilane is more difficult, thermodynamically, than the removal of a second hydrogen atom from tetrasilane.









The Si-H bond from the larger silanes is more reactive, consequently more weak, than the SiH bond in monosilane (Ebsworth, 1963). In other words a hydrogen atom migrates from the  $\text{Si}_5\text{H}_{11}\cdot$  radical in order to produce the stronger bond with  $\text{SiH}_3\cdot$  radicals.

The ions,  $\text{Si}_3\text{H}_6^+$  (m/e = 90) and  $\text{Si}_2\text{H}_4^+$  (m/e = 60) can be formed by two processes, (a) by the equations 6, 9, 10 and 11 or (b) by equations 12, 13 and 14. By either process the ion,  $\text{Si}_3\text{H}_6^+$  (m/e = 90), increases with a decrease in pentasilane and/or the  $\text{Si}_4\text{H}_8^+$  ion (m/e = 120). The process by way of the equations 6, 9, and 10 is supported by the presence of the ion  $\text{Si}_4\text{H}_8^+$  (m/e = 120). However, equation 12 does explain a large ion peak,  $\text{Si}_2\text{H}_4^+$  (m/e = 60). Equation 12 resembles the fragmentation reaction for the paraffins while equation 6 does not. The reaction shown by equation 12 is the reaction predicted by the theory of Lennard-Jones and Hall (see discussion); thereby, it also indicates that the internal Si-Si bonds are weaker than the terminal Si-Si bond.

#### Relative Molar Response for the Silanes

The retention times for the silicon hydrides are given in Table 3. The number of carbon atoms for hydrocarbons have been plotted against the logarithm of the retention time (Desty and Whyman, 1957). The points on the graph can be connected by a straight line. Similarly, a plot of the logarithm of the retention times for silanes versus the number of silicon atoms has been shown to be a straight line (Borer and Phillips,

Table 3. The retention times for the silanes. Flow rate of helium was 80 ml/min. The temperature of the gas chromatograph column was 65°C

Compound	Retention times (min)
monosilane	5.5
disilane	7.4
trisilane	16.2
tetrasilane	53.0
pentasilane	172.3

1959). When the values in Table 3 are plotted in a similar manner, the result is also a straight line.

The relative molar responses for mono- and disilane calculated from experimental data are recorded in Tables 4 and 5. In Table 4, the first column of figures is the pressure in cm of the gases collected in the U-tube. The second column gives the volume of the U-tube. The third column is the number of moles calculated by means of the gas law equation from the pressure and volume given in the first and second columns, respectively. The fourth column is the area of the chromatogram peak measured with a plamineter. The remaining columns give the relative molar responses and the necessary information for the calculation of the standard deviation of the mean value for the relative molar response. In Table 5, the first column gives the pressure in cm of the gases collected in the U-tube. The second column is the number of moles calculated from the gas law equation. The third and fourth columns are the areas of the chromatogram peaks which were measured with a planimeter. The fifth column is the number of moles of monosilane calculated from its area in the third column and its previously calculated relative molar response from Table 4. The sixth column gives the number of moles of disilane remaining after the moles of monosilane in the fifth column have been subtracted from the total number of moles in the second column. The remaining columns give the relative molar response values and the

Table 4. Relative molar response for monosilane

Pressure of the silane in the sample U-tube (cm Hg)	Volume of the sample U-tube (ml)	Moles of silane ( $\times 10^{-6}$ )	Area of silane peak (sq. in.)	RMR of silane	$\Delta$ RMR	$(\Delta$ RMR) <sup>2</sup>
3.51	6.5178	63.99	22.90	43.5	9.2	86.64
1.11	5.9298	3.54	6.00	51.6	1.1	1.21
6.23	6.5178	21.85	11.68	65.1	12.4	153.76
9.93	5.9298	32.01	14.08	53.5	0.8	0.64
4.12	6.5178	14.45	6.06	51.0	1.7	2.89
9.40	5.9298	30.00	26.56	53.9	1.2	1.44
3.25	5.9298	10.37	9.12	53.5	0.8	0.64
34.60	5.9298	110.4	48.46	53.4	0.7	0.49
5.34	5.9298	17.04	8.36	59.7	7.0	49.00
2.70	5.9298	8.62	3.52	49.6	3.1	9.61
1.57	5.9298	5.01	1.98	48.0	4.7	22.09
9.29	5.9298	29.65	21.91	44.9	7.8	60.89
14.17	5.9298	45.23	42.56	57.2	4.5	20.25
				13 ) 684.9	207.55	
Coefficient of variation=10.6				mean value = 52.7 + 5.6		

Table 5. Relative molar response for disilane (Volume of the sample U-tube was 6.5178 ml.)

Pressure of the silane(s) in the sample U-tube (cm Hg)	Total moles of the silanes ( $\times 10^{-6}$ )	Area of mono-silane peak (sq. in.)	Area of di-silane peak (sq. in.)	Moles of monosilane ( $\times 10^{-6}$ )	Moles of disilane ( $\times 10^{-6}$ )	RMR	$\Delta$ RMR	( $\Delta$ RMR)
4.99	15.93	4.24	5.87	8.06	7.87	90.7	14.8	219.04
4.71	15.03	5.60	3.65	10.64	4.39	101.2	4.3	18.49
5.06	15.86	4.03	6.89	7.66	8.20	102.1	3.4	11.56
3.88	12.17	0.00	13.04	0.00	12.17	130.4	24.9	620.01
14.96	47.74	0.00	42.08	0.00	47.74	107.2	1.7	2.89
36.67	117.0	0.00	195.8	0.00	117.0	101.6	3.9	15.21
						633.2		887.20

Coefficient of variation = 11.6

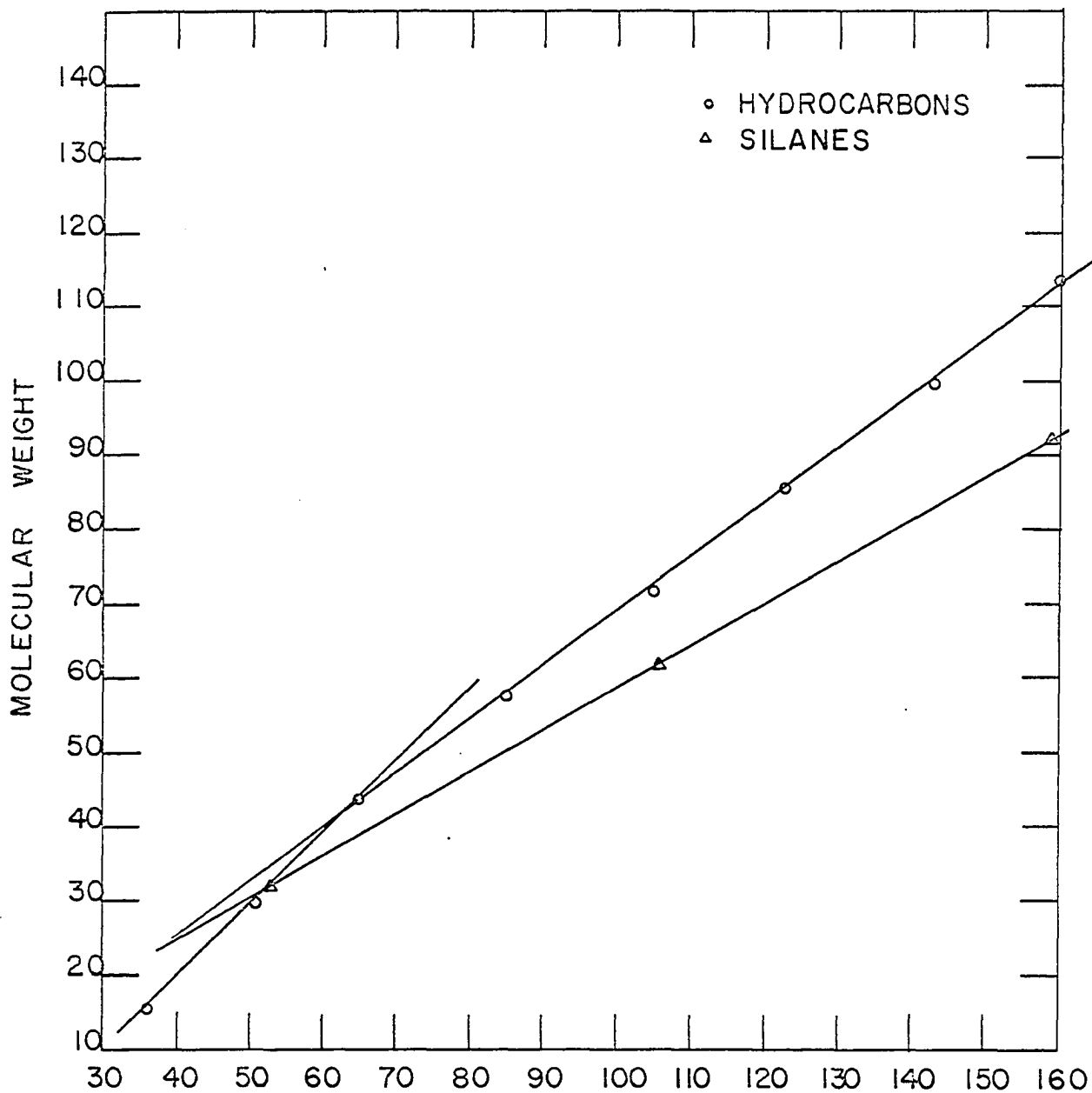
Mean value = 105.5 + 12.2



necessary information for the calculation of the standard deviation of the mean value for the relative molar response. For the measurement of the relative molar response two microliters of benzene, which is equivalent to  $22.5 \times 10^{-6}$  moles, gave an average area of 18.15 square inches for the conditions described in the experimental section of this dissertation. For convenience in the calculations, the average ratio of the moles of benzene to the area of its peak was used. When the relative molar responses for the hydrocarbons are plotted against their molecular weight, a straight line connects the points (Messner, Rosie, and Aragright, 1959) as shown in Figure 28. In order to estimate the relative molar response for trisilane, the assumption was made that the plot of the relative molar responses of the silanes would also be linear. The graph for the plot of the relative molar responses versus the molecular weight for the silanes is given in Figure 28. The relative molar response for trisilane was found by extrapolating the line which connects the points for mono- and disilane to the point corresponding to the molecular weight of trisilane. Its value is 159.

#### Hydrolysis Products of the Rare Earth Silicides

The mole percent of the silanes produced in the reactions of the rare earth silicides with  $6 \text{ N H}_3\text{PO}_4$  are reported in Table 6. The mole percent of silanes produced during the hydrolysis of  $\text{Ce}_5\text{Si}_3$  when the acid concentration was varied is recorded in Table 7. The rate of the reaction increased with temperature.



RELATIVE MOLAR RESPONSE (BENZENE=100)

Figure 28. Relative molar response of n-paraffins and silanes versus molecular weight

Table 6. Results for the hydrolysis of rare earth silicides with 6 N  $H_3PO_4$

Silicide	Area of monosilane peak (sq. in.)	Area of disilane peak (sq. in.)	Area of trisilane peak (sq. in.)	Moles of monosilane ( $\times 10^{-6}$ )	Moles of disilane ( $\times 10^{-6}$ )	Moles of trisilane ( $\times 10^{-6}$ )	Total moles of silanes	Mole % silane	Mole % disilane	Mole % trisilane
$La_5Si_3$	130.6	3.52	0.50	248.1	3.34	0.315	251.76	98.54	1.33	0.13
	192.6	3.12	0.34	365.9	2.96	0.214	369.07	99.14	0.80	0.06
$Ce_5Si_3$	176.0	-	0.21	334.4	- <sup>a</sup>	0.132	334.53	99.96	-	0.04
	119.7	6.66	0.50	227.4	6.31	0.315	234.03	97.17	2.70	0.13
$Pr_5Si_3$	145.3	1.26	-	276.1	1.19	-	277.57	99.57	0.43	-
$Nd_5Si_3$	115.2	14.96	0.65	218.9	14.18	0.409	233.49	93.75	6.07	0.18
	79.36	8.02	0.78	150.8	7.60	0.491	158.89	94.90	4.78	0.32
	104.3	7.40	0.29	198.2	7.02	0.182	205.40	96.49	3.42	0.09
$Gd_5Si_3$	136.6	1.47	-	259.5	1.39	-	260.89	99.47	0.53	-
	146.6	25.92	-	278.5	24.57	-	303.07	91.87	8.11	-
$Dy_5Si_3$	167.0	1.24	-	317.3	1.18	-	318.48	99.63	0.37	-
	139.5	13.56	-	265.1	12.85	-	277.95	95.38	4.62	-
	147.8	8.76	-	280.8	8.30	-	289.10	97.13	2.87	-
$Er_5Si_3$	145.3	0.78	-	276.1	0.74	-	276.84	99.73	0.27	-
	386.6	3.84	-	734.5	3.64	-	738.14	99.50	0.50	-

<sup>a</sup>The disilane probably decomposed since the reaction vessel was heated to dryness before the products were collected.

Table 7. Hydrolytic reactions of  $Ce_5Si_3$  with changes in acid concentration ( $H_3PO_4$ )

Acid concentration	Area of monosilane (sq. in.)	Area of disilane (sq. in.)	Area of trisilane (sq. in.)	Moles of monosilane ( $\times 10^{-6}$ )	Moles of disilane ( $\times 10^{-6}$ )	Moles of trisilane ( $\times 10^{-6}$ )	Total moles ( $\times 10^{-6}$ )	Mole % silane	Mole % disilane	Mole % trisilane
water	117.8	0.54	-	223.8	0.51	-	224.3	99.77	0.23	-
2N	117.8	0.86	-	223.8	0.82	-	224.6	99.63	0.37	-
4N	92.2	5.22	0.67	175.2	4.95	0.421	180.6	97.03	2.74	0.23
6N	176.0	-	0.21	334.4	-	0.132	334.5	99.96	-	0.04
	119.7	6.66	0.50	227.4	6.31	0.315	234.0	97.17	2.70	0.13
8N	141.4	1.12	-	268.7	1.06	-	269.8	99.61	0.39	-
	127.4	0.78	-	242.1	0.739	-	242.8	99.70	0.30	-
10N	115.8	2.22	-	220.0	2.10	-	222.1	99.05	0.95	-

## DISCUSSION

## Relative Molar Response

The detector of the gas chromatograph has two separate compartments. One contains a tungsten filament. The other one contains a matching reference filament. Helium flows constantly through the compartment which houses the reference filament while a mixture of the sample and helium flows through the other compartment. The matching reference filament is opposed to the tungsten filament in a Wheatstone circuit by which the change in resistance of the tungsten filament is measured. Since the resistance of a tungsten filament is dependent on its temperature, the change in its resistance is a measure of the heat conducted from the filament by the sample. A measurement of the heat loss from the filament is directly related to the change in the concentration of the eluate per unit volume of helium as it emerges from the chromatograph column. The exact measurement of heat loss from the filament is difficult. This requires a knowledge of (a) the dimensions of the filament and cell, (b) the thermal conductivities of the samples, and (c) the temperature differential between the cell and the filament. These quantities are interdependent and variable. For example, one of the equations reported by Dal Nogare and Juvet (1962) for the relationship between the response of the detector and the thermal conductivities of the gases is:

$$\frac{\Delta T_f}{x} = \Delta T \left( \frac{k_g}{k_s} - 1 \right) \quad (18)$$

where  $\Delta T_f/x$  = specific cell response,

$k_s$  = thermal conductivity of the solute,

$k_g$  = thermal conductivity of the carrier gas,

$\Delta T$  = temperature difference between the filament  
and the cell wall and

$x$  = mole fraction of solute.

The quantity in parentheses is referred to as the thermal conductivity factor (TC). In order to estimate the cell response, the thermal conductivities of the gases must be known before the thermal conductivity factor can be calculated. A mathematical relationship has not been discovered by which the exact calculation of the thermal conductivity can be made. An approximate relationship is

$$\frac{k_1}{k_2} = \frac{M_2}{M_1} \quad (19)$$

where  $M$  = the molecular weight and

$k$  = thermal conductivity.

According to this equation, the thermal conductivity decreases rapidly for the first few members of an homologous series. For the higher members of an homologous series the thermal conductivity tends to approach a limiting value. The smaller molecules have larger thermal conductivities. (If a small and a large molecule absorb equal amounts of energy from a hot surface, the small molecule has a larger velocity and reaches

a cooler surface sooner than the large molecule.) At any rate the thermal conductivity (TC) can only be approximated. Because of this, along with other variables present in the detector, quantitative methods are not conveniently applicable. Attempts have been made to eliminate the variables by comparing the thermal conductivities of the sample against the thermal conductivity of an internal standard such as benzene. For instance, the ratios of the TC of a gas relative to the TC of a benzene-helium mixture have been considered but the results are only fair. A more accurate method is based on sensitivity factors. If the sensitivity of the detector were the same for all compounds, then the fraction of the peak area for component A divided by the total peak area of all the compounds in the original sample would be the same as the mole fraction for component A. Since the sensitivities for the compounds are not the same, the area percent of component A cannot be assumed to be numerically equivalent to the mole percent of A in the original sample. There is not a one-to-one correspondence between area and moles. The sensitivity factors convert peak areas to correspond to the actual moles introduced into the chromatograph. Rosie and Grob (1957) determined the sensitivity factors for the hydrocarbons. By an internal standard method they determined the detector response per mole of hydrocarbon relative to the response per mole for benzene. The sensitivity factors, called the relative molar responses, RMR, are independent of the gas flow rate, the sensing device, the temperature, and

the concentration (Messner, Rosie and Aragrigh, 1959). The relative molar response is directly proportional to the molecular weight and inversely proportional to the thermal conductivity (see Table 6). The coefficient of variation for the relative molar response for the silanes is greater than that reported for the hydrocarbons (Rosie and Grob, 1957). This may be attributed to a decomposition of the silanes on the filament.

Table 8 illustrates the trend in thermal conductivities and relative molar responses for some of the paraffins and silanes. The thermal conductivity for the hydrocarbons are from the report by Roger A. Svehla (1962). They were calculated from experimentally available viscosity data. The thermal conductivities for the silanes, on the other hand, were estimated from statistical thermodynamics and theoretical viscosity equations given in the Appendix. A silane and a paraffin which have the same molecular weight have approximately equivalent relative molar responses. Within homologous series, such as silanes or paraffins, the relative molar response increases and the thermal conductivity decreases with increasing molecular weight. The equation used for the calculation of the thermal conductivity contains a term which includes the heat capacity. The thermal conductivity for trisilane was not calculated since its heat capacity could not be estimated.



Table 8. Thermal conductivities and RMR for straight chained hydrocarbons and silanes at 300 °K

Compound	Molecular Weight	Thermal conductivity ( $\times 10^6$ ) g-cal/(cm) (sec) (°K)	RMR
methane	16	85.0a	36
ethane	30	54.2 <sup>a</sup>	51
propane	44	43.3 <sup>a</sup>	65
butane	58	41.0 <sup>a</sup>	85
pentane	72	38.9 <sup>a</sup>	105
benzene	78	25.9 <sup>a</sup>	100
monosilane	32	53.0 <sup>a</sup> (46.7) <sup>b</sup>	52
disilane	62	35.5 <sup>b</sup>	106
trisilane	92	-	(159) <sup>c</sup>

<sup>a</sup>The value was calculated from viscosity data by Roger A. Svehla (1962)

<sup>b</sup>The value was calculated from force constants as shown in the appendix.

<sup>c</sup>The value was determined by the linear extrapolation of the values for monosilane and disilane. See Figure 28 .

## Mass Spectra of the Silanes

No simple or accurate method has been invented to calculate the mass spectra of all molecules in terms of a priori assumptions. Two theories which have been proposed are based on the molecular orbital theory of chemical valencies and the quasi-equilibrium rate theory. Lennard-Jones and Hall (1952) applied the molecular orbital theory for the calculation of the ionization potential for the paraffins. In order to do this, they had to calculate the distribution of a resultant positive charge among atoms after an electron was removed from a molecular orbital. The fraction of the positive charge residing on each carbon atom was calculated by squaring the coefficients of the carbon-carbon orbitals. They postulated that the weakest bond remaining after the ionization of the molecule would be the bond with the largest accumulation of a positive charge. In the derivation for the calculation of the ionization potential, Lennard-Jones (1949) found that a more convenient description for an ionized molecule involved introducing "equivalent orbitals". Molecular orbitals belong to irreducible representations of the symmetry group which involve the molecule as a whole. They are convenient for discussion of properties such as excitation or ionization of a molecule by light. Equivalent orbitals are identical members of the same symmetry group except for orientation and position in space. They described localized properties of the molecule such as charge distribution

in bonds. They are the quantum mechanical analogue of localized chemical bonds, lone pairs or inner shells. The equivalent orbital method is based on the assumption that the electronic wave functions of a molecule can be expressed as a matrix  $e_{mn}$  of mutually orthogonal equivalent orbitals, each involving the co-ordinates of one electron only. The matrix can be transformed to give a diagonal matrix  $E_{ij}$ . The diagonal elements  $E_{nn}$  of the matrix  $E_{ij}$  then represent the vertical ionization potentials of the electrons in the corresponding molecular orbitals (Lennard-Jones and Hall, 1949). The matrix elements in  $e_{mn}$  represent the interaction parameter between atoms with respect to two equivalent orbitals  $X_m$  and  $X_n$  of the self-consistent Hamiltonian  $H$ . The matrix can be represented by the equation

$$e_{mn} = \int \bar{X}_m (H + V + A) X_n d\tau \quad (20)$$

where

$$V = \sum_n \int \bar{\psi}_n (1/r_{12}) \psi_n d\tau$$

$$A \psi_i = -\sum_n \int \bar{\psi}_n (1/r_{12}) \psi_n d\tau \psi_i$$

The change in the interaction parameters due to the alteration of a neighboring orbital, often referred to as an inductive effect, was avoided by assuming that chemically equivalent orbitals have equal interaction parameters as if they were mathematically equivalent, i.e. chemically equivalent orbitals

are surrounded by the same immediate neighbors.

In order to find the ionization potential and molecular orbitals from known equivalent orbitals, a matrix for which

$$e_{il} = \sum_l T_{il} \chi_l$$

must be found. The transformation of the matrix  $e_{mn}$  follows

$$E_{ij} = \sum_m T_{mi}^{-1} e_{mn} T_{jn} \quad (21)$$

Such a matrix  $T_{il}$  for the diagonalization of  $e_{mn}$  is determined by solving the eigenvalue equations. In other words the roots are determined for the secular determinant associated with the variation theorem. The determinant is

$$|e_{mn} - E\delta_{mn}| = 0 \quad (22)$$

The roots,  $E_{nn}$ , represent the ionization potentials and the molecular orbitals are found from the corresponding eigenvectors determined for the required matrix  $T_{il}$ . On the basis of a semi-empirical method the matrix elements for  $e_{mn}$  are calculated from the lowest, observed ionization potentials for methane and ethane. These constants are then used in the calculation of the ionization potentials for larger saturated molecules. The expansion of the molecular orbitals of the paraffins in terms of equivalent carbon-carbon orbitals is shown by Lennard-Jones and Hall (1952) to be

$$R_{2n} = R \sin \frac{2nr\pi}{2s} \quad (23)$$

where  $r = 1, 2, 1, \dots, s$ , and  $s =$  number of carbon atoms.

The fragmentation pattern is proportional to the  $(R_{2n})^2$  terms. The fragmentation pattern of n-octane at 50 eV parallels the charge densities on the different carbon-carbon bonds (Thompson, 1953). However, Coggeshall (1959) showed that the series increases proportionally by  $2 \sin \frac{2n\pi}{S}$ , where n is the number of carbon atoms starting with a terminal atom ( $n = 1$ ) and increasing to the center atom ( $n = s$ ). The maximum value occurs at approximately one-half the molecular weight. The mass spectra for paraffins larger than n-octane have large ion peaks for  $C_3$  and  $C_4$  fragments. Coggeshall (1959) thus proved that the above method was not applicable to all paraffins. Lorquet (1966) suggested that the charge is too evenly distributed over the large paraffin molecules for decisive influence on the fragmentation patterns. He also improved the above theory by considering the inductive effects and the modification of the molecular orbitals subsequent to ionization.

The calculation of mass spectra according to the quasi-equilibrium theory is based on the assumption that the ionization of a molecule by electron impact is a Franck-Condon transition. (The equilibrium distances between the atoms of a molecule in its ground molecular state are not the same as those in its ground ionic state. A vertical line from the minimum point of the potential energy curve for the ground molecular state to the potential energy curve for the ground ionic state intersects the potential energy curve for the ion

at a point above the ground ionic state. The vertical line represents the removal of a valence electron from a molecule without any change in its internuclear distances. The process is called a vertical transition or a Franck-Condon transition. The process of ionizing a molecule from its ground molecular state to its ground ionic state along a non-vertical line is known as an adiabatic transition.) As a result the ion has excess energy above the ground ionic state. The quasi-equilibrium theory assumes that the excess energy is randomly distributed as vibrational energy throughout the ion before it decomposes. In other words the molecule becomes an activated ion before it decomposes to the final fragments. Therefore, the molecular processes are a series of competing, consecutive, unimolecular decompositions. For this reason the quasi-equilibrium theory states that a mass spectrum is not the initial fragmentation pattern.

If the assumptions are made that the equivalent orbital theory can be used to explain the mass spectra of molecules and that the equivalent orbitals used in the calculations for the paraffins are analogous to the equivalent orbitals in the silanes, then the main fragment of the mass spectra of the silanes should have a mass approximately one-half the corresponding molecular weight. From the results for the mass spectra of the silanes observed in this research, the theory of Lennard-Jones and Hall does approximately apply since the major ion peak for the fragmentation pattern for

disilane, trisilane, tetrasilane and pentasilane occurred at  $m/e = 60$ . However, the mass spectra for tetrasilane and pentasilane changed with time, i.e. they decomposed. The kinetics and energies involved in the fragmentation of these silanes are certainly important factors for the explanation of their mass spectra.

#### Hydrolysis Reactions of the Rare Earth Silicides

Silicon, like carbon, has four valence electrons which occupy s and p orbitals. The chemical properties of elements which have the same number of valence electrons are usually quite similar. The chemistry of silicon, however, cannot be, as a rule, inferred from that of carbon. There are two striking differences between the two elements, the ability for catenation and the formation of double and triple bonds by the carbon atoms. For many years the bonds of carbon have been explained by the hybridization of the atomic orbitals, i.e. an s electron is promoted to a p orbital and the four orbitals are mixed to form four equivalent  $sp^3$  orbitals. In addition,  $sp$  and  $sp^2$  hybrids can form. These hybrid orbitals are speculated in the formation of multiple bonds. For example, if two  $sp^2$  hybrid orbitals on adjacent carbon atoms are so directed that a maximum overlap of the orbitals results in the formation of a bond, the remaining p orbitals which lie in the same plane and are not used in the hybridization are close enough to overlap with one another to form a  $(p-p)\pi$  bond. In comparison, the distance between adjacent silicon

atoms with an overlap of two  $sp^2$  orbitals to form a sigma bond is too great to permit the overlap of the two adjacent remaining p orbitals in order to form a  $\pi$  bond. The reason for the large distance between silicon atoms is the repulsion of inner shell non-bonded electrons under the valence shell of the silicon atoms. Carbon has only 2 inner shell electrons per atom while silicon has 10; therefore, carbon atoms are able to approach closer to one another. Consequently, the absence of multiple bonds in the silicon hydrides from the hydrolyses is not surprising. On the other hand the silicon atom does have available d orbitals where as the carbon atom does not. If an atom with a great enough electronegativity is bound to a silicon atom, the d orbitals can contract to such an extent that they are available for the formation of bonds. In fact, the change from the unstable silicides of the electropositive metals to the stable refractory compounds of the transition metals occurs where the overlap of the d or f - and s- orbitals of the metals is possible, thus, forming more stable bonds.

The Si-Si bond is weaker than the C-C bond and this fact probably contributes to the inability for the silicon to link with itself to form long chains. However, the ionicity of the bond and the rest of the molecule must also be considered. For example, the Si-Cl bond is stronger, yet more reactive, than say the Si-C bond. The greater shift in the polarity of the Si-Cl electrostatic charges on the atoms due to the



greater electronegativity of Cl compared to C delocalizes the electrons to give a small positive charge to the silicon atom. The silicon atom is susceptible to an electrophilic attack by a hydride ion as noted in the hydrolytic reactions.

Kachi and Kanno have investigated the relationship between the crystalline structure and chemical bonding of the carbides, and the hydrolysis products. They observed the following correlations:

(a) The hydrolysis of the monocarbides of UC and ThC which have a NaCl structure produces methane. This is expected since metal atoms prevent bonding between carbon atoms in the carbides and thereby the occurrence of C-C bonds in the products is less likely.

(b) The hydrolysis of the dicarbides,  $\text{LaC}_2$  and  $\text{CeC}_2$ , give acetylene which can be expected since the dicarbides have structures similar to NaCl if the C-C linkages are each considered a single group.

(c) The degree of single, double and triple bond character of the  $\text{C}_2^{2-}$  units in the crystalline structure were calculated from the mole fraction of the products methane, ethene and acetylene formed during hydrolysis. The distance for the C-C bond calculated from the hydrolysis products agreed with the C-C distance determined experimentally by crystallography. The C-C distance for  $\text{LaC}_2$  and  $\text{CeC}_2$  lies between the C-C distances for double and triple bonds.

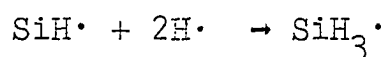
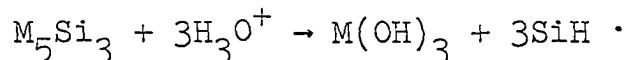
The results from the hydrolysis of the rare earth silicides are summarized below.

- (a) Monosilane is the major product in all reactions.
- (b) Intermediate rare earth silicides produce the largest relative amount of disilane.
- (c) Temperature and acid strength increase the rate of hydrolysis.
- (d) The lighter rare earth silicides produce some trisilane while the heavier rare earth silicides do not.
- (e) An acid concentration between 4 and 6 N produces the largest yield of trisilane in the case of the hydrolysis of  $Ce_5Si_3$ .
- (f) The hydrolytic reactions did not produce tetra- or pentasilane.

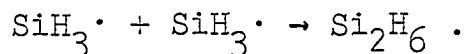
The bond lengths for Si-Si, M-Si and M-M have not been reported for the rare earth silicides,  $M_5Si_3$ . For a similar structure,  $Ta_5Si_3$ , the bond lengths are 3.08Å, 2.61Å and 2.56Å for the bonds Si-Si, Ta-Ta, and Ta-Si, respectively (Nowotny, 1955). If the assumption is valid that the bond lengths for the rare earth silicides,  $M_5Si_3$ , are approximately the same as those reported for  $Ta_5Si_3$ , then the Si-Si bond in the silicides is assuredly longer than the Si-Si bond in disilane. (The length of the Si-Si bond in disilane is  $2.330 \pm 0.005\text{Å}$ .) (Svec and Saalfeld, 1966 p. 1755). Disilane probably does not form by a direct hydrolytic mechanism on the silicides surface but rather it is formed by the

combination of silyl radicals.

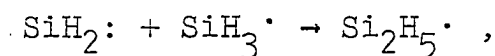
The rare earth silicides of the structure  $M_5Si_3$  probably have ionic character. Since silicon is more electronegative than the rare earth elements, the silicon atom can be expected to have a small negative charge surrounding it. A hydronium ion is attracted to the surface of the silicide by the electrostatic force of the silicon atom, so much so in fact, that some of the silicon atoms break metal-silicon bonds to form radicals with the hydrogen. A typical reaction might be



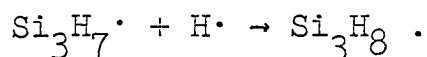
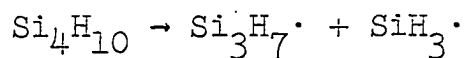
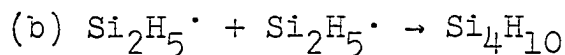
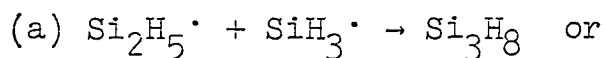
Once the silyl radicals are formed, they may produce disilane by the following combination



If disilyl radicals are formed by the reaction



the formation of trisilane can occur by two processes which are



## SUMMARY

The silicides,  $\text{La}_5\text{Si}_3$ ,  $\text{Ce}_5\text{Si}_3$ ,  $\text{Pr}_5\text{Si}_3$ ,  $\text{Nd}_5\text{Si}_3$ ,  $\text{Gd}_5\text{Si}_3$ ,  $\text{Dy}_5\text{Si}_3$  and  $\text{Er}_5\text{Si}_3$ , were prepared by direct combination of the elements in an arc melter under an atmosphere of argon. They were hydrolyzed with 6 N  $\text{H}_3\text{PO}_4$ . In all of the reactions monosilane (95 mole percent or more) and disilane (5 mole percent or less) were produced. Trisilane was formed by the hydrolysis of  $\text{La}_5\text{Si}_3$ ,  $\text{Ce}_5\text{Si}_3$  and  $\text{Nd}_5\text{Si}_3$  but it was not observed for the hydrolysis of  $\text{Pr}_5\text{Si}_3$ ,  $\text{Dy}_5\text{Si}_3$ ,  $\text{Gd}_5\text{Si}_3$  and  $\text{Er}_5\text{Si}_3$ . No tetra- or pentasilane was produced in any of the reactions. The hydrolytic reactions for  $\text{Ce}_5\text{Si}_3$  were studied as a function of the acid concentration. When  $\text{Ce}_5\text{Si}_3$  was hydrolyzed with water, 2 N, 8N or 10 N  $\text{H}_3\text{PO}_4$ , only monosilane and disilane were formed. For 4 N and 6 N  $\text{H}_3\text{PO}_4$ , trisilane was also observed.

The silanes were separated by means of a gas chromatograph and identified with a mass spectrometer. In order to calculate a more accurate value for the number of moles of silanes from the area of the chromatogram peaks, the sensitivity factors (relative molar responses) of the chromatograph detector were determined. The values for the relative molar responses for monosilane and disilane were  $52.7 \pm 5.6$  and  $105.5 \pm 12.2$ , respectively (benzene = 100). The relative molar response for trisilane was estimated from the relative molar responses of monosilane and disilane to be 159.

## BIBLIOGRAPHY

- Andrieux, Jean L.  
1938 Binary alloys or compounds produced by fused salt electrolysis (translated title). *Congres de Chimie Industrielle, Comptes Rendus 18me Congress, Nancy 1938*: 124.
- Aronsson, B., T. Lundstrom and S. Rundqvist.  
1965 Borides, silicides and phosphides. New York, N.Y., John Wiley and Sons, Inc.
- Atoji, M., Karl Gschneidner, Jr., A. H. Daane, R. E. Rundle and F. H. Spedding.  
1958 The structures of lanthanum dicarbide and sesquicarbide by X-ray and neutron diffraction. *Journal of American Chemical Society* 80: 1804.
- Ban, Z. and M. Sikirca.  
1963 Crucible-free synthesis of silicates and borides. In *Proceedings of the Conference on New-Nuclear Materials Including Non-Metallic Fuels. Vol. 2. p. 175. Vienna, Austria, International Energy Agency. 1963.* Original not available; abstracted in *Chemical Abstracts* 60: 10,192h 1964.
- Boltzmann, L.  
1872 Further studies on the thermal equilibrium among gas-molecules (translated title). *Berichte der Deutschen Chemischen Gesellschaft* 66: 275.
- Borer, K. and C. S. G. Phillips.  
1959 The separation of volatile silanes and germanes by gas-liquid chromatography. *Proceedings of the Royal Chemical Society (London)* 1959: 189.
- Buff, H. and F. Wohler.  
1857 *Justus Liebigs Annalen der Chemie* 103: 218.
- Callery Chemical Company.  
ca. 1950 Uncertified mass spectrum: silane, Parent Mass 32. Callery, Pennsylvania, Callery Chemical Company.
- Chapman, S.  
1911 The theory of viscosity and thermal conduction (translated title). *Philosophical Transactions of the Royal Society (London) Series A*, 216: 279.

- Chapman, S.  
1916 On the law of distribution of velocities, and on the theory of viscosity and thermal conduction, in a non-uniform simple monatomic gas. Philosophical Transactions of the Royal Society (London) Series A, 216: 279.
- Clausius, R.  
1862 Uber die Warmeleitung gas formiger Korper. Poggendorf Annalen der Physik 115: 1.
- Coggeshall, N. D.  
1959 Ionization of n-paraffin molecules. Journal of Chemical Physics 30: 595.
- Cox, A. Peter.  
1965 Private communication of unpublished results. Department of Chemistry, The University, Bristol 8, England.
- Dal Nogare, S. and Richard S. Juvet, Jr.  
1962 Gas-liquid chromatography. New York, N.Y., Interscience Publishers.
- Damiens, A.  
1913 Etude de l'action de l'eau sur les carbures des terres rares. Comptes Rendus Hebdomadaires des Seances de l'Academie des Sciences 157: 214.
- Desty, D. H. and B. H. F. Whyman.  
1957 Application of gas-liquid chromatography to analysis of liquid petroleum fractions. Analytical Chemistry 29: 320.
- Deville, H. S. C. and H. Caron.  
1857 Memoire sur le silicium et les siliciures metalliques. Comptes Rendus Hebdomadaires des Seances de L'academie des Sciences 157: 214.
- Ebsworth, E. A. V.  
1963 Volatile silicon compounds. New York, N.Y., Pergamon Press.
- Electroschmelzwerk Kempton.  
1963 Arc-furnace smelting without slag. British Patent 924,566. April 24, 1963. Original not available; abstracted in Chemical Abstracts 59: 302g.

- Enskog, D.  
1917 The kinetic theory of phenomena in fairly rare gases. Unpublished dissertation. Upsala. Original not available; cited in Chapman, S. and T. G. Cowling. The mathematical theory of non-uniform gases. p. 3894. Cambridge, England, The University Press 1964.
- Enskog, D.  
1922 Kinetic theory of thermal conduction, viscosity, and self-diffusion in certain dense gases and liquids. Svenska Akademiens Handlingar No. 4: 63.
- Eucken, A.  
1913 Über das Wärmeleitvermögen, die spezifische Wärme und die innere Reibung der Gase. Physikalische Zeitschrift 14: 324.
- Feher, F. and W. Tromm.  
1955 Die Darstellung von Silanen aus Magnesiumsilicid und Hydrazoniumchlorid in wasserfreiem Hydrazin. Zeitschrift für Anorganische und Allgemeine Chemie 282: 29.
- Finholt, A. E., A. G. Bond, K. E. Wilzbach and H. L. Schlesinger.  
1947 The preparation and some properties of hydrides of elements of the fourth group of the periodic system and of their organic derivatives. Journal of the American Chemical Society 69: 2692.
- Forsyth, J. S. A.  
1941 The reaction of free methyl radicals with nitric oxide. Transactions of the Faraday Society 37: 312.
- Gekhale, S. D., J. E. Drake and W. L. Jolly.  
1965 Synthesis of higher silanes and germanes. Journal of Inorganic and Nuclear Chemistry 27: 1911.
- Gladyshevskii, E. I. and P. I. Kripyakevich.  
1963 Monosilicides or rare earth metals and their crystal structures (translated title). Zhurnal Strukturnoi Khimii 5: 853.
- Greenwood, N. N. and A. J. Osborn  
1961 Chemical and magnetic properties of lanthanum dicarbide and sesquicarbide. Journal of the Chemical Society (London) 1961: 1775.
- Hall, G. G.  
1951 The molecular orbital theory of chemical valency. VIII. A method of calculating ionization potentials.

Proceedings of the Royal Society (London) Series A,  
205: 541.

Harper, L. R., S. Yolles and H. C. Miller.

1961 Decomposition of disilane-separation of silane/  
disilane mixtures by gas phase chromatography.  
Journal of Inorganic and Nuclear Chemistry 21: 294.

Hirschfelder, Joseph, Charles F. Curtiss and R. B. Bird.

1954 Molecular theory of gases and liquids. New York,  
N. Y., John Wiley and Sons, Inc.

Hsu, S. S., P. N. Yocum, T. C. C. Cheng, K. B. Oldham

C. E. Meyers, Karl Ginerich, C. H. Travaglini, Y. C. Bailar, Jr.,  
H. A. Laitinen and Sherlock Swann, Jr.

1961 Preparation and properties of phosphides and silicides  
and some electrochemical studies. U. S. Department  
of Commerce, Office of Technical Service, P. B.  
Report No. 147,079. Original not available;  
abstracted in Chemical Abstracts 56: 12,664i.

Johnson, Warren C. and Sampson Isenberg.

1935 Hydrogen compounds of silicon. I. The preparation of  
mono- and disilane. Journal of the American Chemical  
Society 57: 1349.

Kanno, K. and S. Kachi.

1962 The relationship between the crystal structure of  
various carbides of thorium, uranium and rare earth  
elements and the products obtained when these carbides  
are hydrolysed (translated title). Journal of Chemical  
Society of Japan (Nippon Kagaku Zasshi) 83: 565.

Kosolopova, T. Y., O. V. Kaminskaya, N. A. Kovalekno and  
L. T. Pustovoit.

1965 The hydrolysis of the rare earth carbides (translated  
title). Zhurnal Neorganicheskoi Khimii 10: 2453.

Latva, John D.

1962 Selection and fabrication of nonmetallic-oxides,  
beryllides and silicides. Metal Progress 82, No. 5: 97.

Lennard-Jones, Sir. John.

1949 The molecular orbital theory of chemical valency. I.  
The determination of molecular orbitals. Proceedings  
of the Royal Society of London. Series A, 198: 1.

Lennard-Jones, Sir John and G. G. Hall.

1952 Ionization of paraffin molecules. Transactions of  
Faraday Society 48: 581.

Lorquet, J. C.

1966 A theoretical study of the ionization of alkanes. In



Mean, W. L., ed. Advances in mass spectrometry.  
Vol. 3. pp. 443-449. London, England, The Institute  
of Petroleum.

- Maxwell, J. C.  
1867 On the dynamical theory of gases. Philosophical  
transactions of the Roy Society 157: 49.
- Messner, A. E., D. M. Rosie and P. A. Aragrighu.  
1959 Correlation of thermal conductivity cell response  
with molecular weight and structure. Analytical  
Chemistry 31: 230.
- Moissan, H.  
1920 The electric furnace. Easton, Penn., Chemical  
Publishing Co.
- Moissan, H. and S. Smiles.  
1902 Sur quelques propriétés nouvelles du silicium  
amorphe. Comptes Rendus Hebdomadaires des  
Seances de l'Académie des Sciences 134: 1552.
- Nowotny, H., E. Parthe and B. Lux.  
1955 Der Aufbau der Silizide  $M_5Si_3$ ; Monatschrift 86: 859.
- Palenik, G. J. and J. C. Warf.  
1962 Hydrolysis of La and Ce carbides. Inorganic chemistry  
1: 683.
- Phillips, C. S. G. and P. L. Timms.  
1963 Some applications of gas chromatography in inorganic  
chemistry. Analytical Chemistry 35: 505.
- Phillips, C. S. G. and P. L. Timms, and C. C. Simpson.  
1964 The silicon-germanium hydrides. Journal of the  
Chemical Society (London) 1964: 1467.
- Pollard, F. H., C. Nickless and S. Evered.  
1963 Chromatographic studies on the hydrolysis of carbides.  
Part I. The preparation and hydrolysis of rare earth  
dicarbides. Journal of Chromatography 15: 211.
- Pupezin, Jovan D. and Kiro F. Zmbov.  
1958 Mass spectrometric investigation of silicon hydrides.  
Bulletin of the Institute of Nuclear Sciences "Boris  
Kidrich" 8, No. 154: 89.
- Rosie, D. M. and Robert L. Grob.  
1957 Thermal conductivity behavior. Analytical Chemistry  
29: 1263.

- Samsonov, G. V., M. S. Koval'chenko and T. S. Verkhoglyadova.  
1959 Preparation of the disilicides of high-melting metals.  
Russian Journal of Inorganic Chemistry 4: 1276.
- Sansonov, G. V. and V. S. Neshpor.  
1960 Alloys of the rare metals with boron and silicon for  
certain radio and electrical applications. Redkie  
Metally i Phlaooy, Trudy Pervago Vsesoyunznogo  
Soveshchaniya po Splavam Redkikh Metallov. (Rare  
Metals and Alloys, Transactions of the First All-  
union Conference on Alloys of Rare Metals.)  
Metallurgisdat. A. A. Baikova pp. 392-417. Original  
not available; translation secured from Joint  
Publication Research Service, Washington, D. C. 1963.
- Stern, David R. and Quentin H. McKenna.  
1960 Metal borides and silicides. United States Patent  
29,936,268. May 10, 1960. Original not available;  
abstracted in Chemical Abstracts 55: 3247b.
- Stock, A. and C. Somieski.  
1916 Silicium wasserstoffe. I. Die aus Magnesiumsilicid  
und Sauren entstehenden Silicium wasserstoffe.  
Berichte der Deutschen chemischen Gsesllschaft  
49: 111.
- Stock, A. and C. Somieski.  
1919 Silicium wasserstoffe. Vi. Chlorierung and  
Methylierung des Monsilanes. Berichte der Deutschen  
chemischen Gesellschaft 52: 695.
- Stone, F. G. A.  
1962 Hydrogen compounds of the group IV elements. Engle-  
wood Cliffs, N. J., Prentice-Hall, Inc.
- Sparrow, G. R. and H. J. Svec  
1966 An analytical treatment of ionization effeciency data  
for xenon from a pulsed retarding-potential ion source.  
Unpublished Ph.D. thesis. Ames, Iowa, Library,  
Iowa State University of Science and Technology. 1960.
- Svec, H. J., J. Capellen and Fred E. Saalfeld.  
1964 The hydrolysis of the rare-earth carbides.  
Journal of Inorganic and Nuclear Chemistry 25: 721.
- Svec, H. J., and Freed Saalfeld.  
1963 The mass spectra of volatile hydrides. II. Some  
higher hydrides of Group IV B and VB elements.  
Inorganic Chemistry 2: 49.

- Svec, H. J. and Fred Saalfeld.  
1966 Mass spectra of volatile hydrides. IV. Silylgermane.  
Journal of Physical Chemistry 70: 1753.
- Svehla, Roger A.  
1962 Estimated viscosities and thermal conductivities of  
gases at high temperatures: NASA TR-R-132.  
Cleveland, Ohio, Lewis Research Center.
- Thompson, R.  
1953 Conference on applied mass spectrometry. London,  
England, Institute of Petroleum 1953: 154.
- Villelume, J. De  
1951 Action de la vapeur d'eau sur le carbure de lanthane.  
Comptes Rendus Hebdomadaires des Seances de L'academie  
des Sciences 232\_ 235.
- Wells, A. F.  
1962 Structural inorganic chemistry. 3rd ed. Oxford,  
England, The Clarendon Press.
- Wilson, M. K. and George W. Bethke  
1957 Vibrational spectrum of disilane. Journal of  
Chemical Physics 26: 1107.
- Wohler, F.  
1858 Ueber das Silicium-Mangan. Gesellschaft der  
Wissenschaften zu Gottengen 1858: 59.

## ACKNOWLEDGMENTS

The author wishes to thank Dr. Harry J. Svec for his guidance, patience and interest during the completion of this research. He finds that his discussions with Dr. Svec have been informative not only along the lines of scientific thought but also on the responsibilities of a scientist and on the correct usage of the English language.

He thanks the men in the maintenance shop and in the glass shop for their aid in the construction and repair of numerous items necessary for the completion of this research.

He wishes to express his gratitude to the members of Physical and Inorganic Chemistry Group VII for their cooperation and helpful suggestions concerning this project. He is particularly grateful to Harold Belsheim, who was willing to read the manuscript for errors and who also gave the author a better understanding of chemistry.

He offers gratitude to his typist, Mrs. Paula Toms, for providing services beyond that of typing this manuscript.

He is indebted to Dr. Gene Sparrow for his assistance in obtaining the mass spectra of the silanes and for his loyal friendship.

He thanks Earleen DeLay, a cousin, whose financial aid and personal encouragement enabled him to complete his freshman year as an undergraduate in college.

Finally, he expresses his thanks for Marge.

## APPENDIX

Calculations for the Thermal Conductivities of the Silanes

The mechanism of heat conduction has been explained in terms of the kinetic theory of gases. A gas is composed of small, constantly moving, uniform particles called molecules which are separated by an average distance larger than their diameter. The thermal energy of a moving molecule is the summation of its rotational, vibrational, and translational motion. The interaction or collision of molecules with one another is a means by which energy (heat) is transported. If a gas is separated by two parallel plates, each maintained at a different temperature, molecules which collide with the hotter plate acquire thermal energy and as a result have an increase in velocity. A molecule can exchange its kinetic energy to other molecules in collisions until the energy originally absorbed from the hotter plate is communicated to the cooler plate. The net result is a transport of thermal energy. The phenomena is known as thermal conductivity. For a monatomic gas, the kinetic energy is exclusively translational energy. For polyatomic gases, the kinetic energy includes rotational and vibrational energy.

Clausius (1862) proposed the calculation of thermal conductivity by the summation of all of the molecules which collide while they pass through a given area per unit of time. His work was the basis for the equation.

$$\lambda = f \frac{r}{\eta} c_v \quad (24)$$

where  $\lambda$  = thermal conductivity,

$\eta$  = viscosity,

$c_v$  = specific heat at constant volume, and

$f$  = correction coefficient.

The correction coefficient is a function of the nature of the gas and is the most difficult variable to define.

Maxwell (1867) and Boltzmann (1872) independently introduced a calculation for thermal conductivities which considered the effect of intermolecular forces on the number of collisions between gas molecules. Their derivations, contained terms relating the rotation of a molecule and the repulsion or attraction between molecules. They assumed that molecules interact at small distances for a very short period of time. Although their equation did show correctly a direct proportion between thermal conductivity and temperature, it did not give satisfactory values for experimental results.

Sutherland derived an expression which related the temperature dependence of the correction coefficient. In his derivation he introduced an equation of motion which defined the path of deflection of a molecule as it approached another. Chapman (1911) was able to calculate values corresponding closer to experimental values by adding more terms to Sutherland's equation. He also applied the Maxwell velocity distribution function assuming that the velocity changes with position. In conjunction with a correction coefficient

expression derived by Enskog (1917), he later developed an equation which was based on the following assumptions (Chapman, 1916). (1) All molecules are solid and freely rotating. (2) Transformation of rotational to translational energy occurs, and vice versa. (3) The radius of a molecule changes with relative velocity of the pair of colliding molecules.

Hirschfelder, Curtiss and Bird (1954) made a detailed analysis of the Enskog-Chapman theory by applying a variational principle. They expressed transfer coefficients in terms of a system of integrals whose values depend on the potential function of intramolecular interactions. In the strictest sense their equation applied only to monatomic gases because their theory was based on the assumptions: (a) that molecules have spherical symmetry, (b) that pair collisions only occur, and (c) that the exchange of internal energy is negligible. Thus for polyatomic molecules they introduced a correction coefficient due to Eucken (1913) which corrected the calculations for translational, rotational and vibrational components of energy. Their equation was used for the calculation of the thermal conductivity for the silanes in this dissertation.

The equation used for the calculation of the thermal conductivity is

$$\lambda \times 10^6 = \frac{R}{M} \left[ 15/4 + 1.32 \left( \frac{C_p}{R} - \frac{5}{2} \right) \right] (\eta \times 10^6) \quad (25)$$

where  $\lambda$  = the summation of the translational and internal thermal conductivities

[g-cal/(cm) (sec) ( $^{\circ}$ K)],

R = gas constant [1.98726 g-cal/(g-mole) ( $^{\circ}$ K)],

M = molecular weight [g/g-mole],

$C_p$  = heat capacity at constant pressure [g-cal/(g-mole) ( $^{\circ}$ K)],

= coefficient of viscosity [g/(cm) (sec)].

When the experimental viscosity was not available, it was calculated from the following equation

$$\eta \times 10^6 = \frac{26.693 \sqrt{MT}}{\sigma^2 \Omega(2,2)^*} \quad (26)$$

where M = molecular weight [g/g-mole],

T = temperature [ $^{\circ}$ K],

$\sigma$  = low-velocity collision diameter [ $\text{\AA}$ ],

$\Omega(2,2)^*$  = reduced collision integral.

The calculation of the reduced collision integral, which depends on the intermolecular forces, are based on the Lennard-Jones (12-6) potential energy for the interaction of colliding gas molecules. The integrals are tabulated as a function of the reduced temperature  $KT/\epsilon$  in Table I-M (Hirschfelder, Curtiss and Bird, 1954, pp. 1126-1127). Thus, it is necessary to know the force constants  $\sigma$  and  $\epsilon/k$  for each kind of molecule. Whenever the data is available, the constants are obtained from measurements for the viscosity and thermal conductivity of the molecule. Otherwise they are estimated from physical properties such as critical constants, boiling points, boiling-point densities, melting-point densities and second virial coefficients.



Specifically, the equations of the line which made a least square fit of accumulated measured values  $\epsilon/k$  versus boiling point and  $\sigma$  versus boiling point molar volume were used.

They are

$$\epsilon/k = 1.18 T_b \quad (27)$$

where  $T_b$  is the boiling point temperature, and

$$\sigma^3 = \frac{3}{2\pi N} (2.0 V_b - 5) \quad (28)$$

where  $N$  is Avogadro's number ( $6.023 \times 10^{23}$  molecules/g-mole) and  $V_b$  is the molar volume at the boiling point ( $\text{cm}^3$ ).

The heat capacity for disilane was estimated by the equation

$$\frac{C_p}{K} = \frac{(\Delta C_p)_t}{K} + \frac{(\Delta C_p)_v}{K} + \frac{(\Delta C_p)_r}{K} + \frac{(\Delta C_p)_e}{K} \quad (29)$$

where  $(\Delta C_p)_t$ ,  $(\Delta C_p)_v$ ,  $(\Delta C_p)_r$ , and  $(\Delta C_p)_e$  are the changes in heat capacity due to translational, vibrational, rotational and electronic energies, respectively.  $K$  is the Boltzmann constant. The changes in heat capacities for the various types of energy were calculated from the equations:

$$\frac{(\Delta C_p)_v}{K} = \frac{5}{2}, \quad (30)$$

$$\frac{(\Delta C_p)_r}{K} = 1, \quad (31)$$

$$\frac{(\Delta C_p)_e}{K} = 0, \text{ and} \quad (32)$$

$$\frac{(\Delta C_p)_v}{K} = \frac{\frac{0.7193}{T} \bar{v}_i}{\sinh\left(\frac{0.7193}{T} \bar{v}_i\right)} \quad (33)$$

The wave number ( $\bar{v}_i$ ) for the different modes of vibration were taken from the report by Wilson and Bethke (1957).